Forever young: how AHL15 delays developmental phase transitions to prevent ageing in plants

Luden, T.

Chapter 2

Insights into polycarpic plant development through natural variation in the aerial rosette phenotype in *Arabidopsis thaliana*

Thalia Luden[1], Marieke Koekkoek[1], Remko Offringa[1]

[1] Plant Developmental Genetics, Institute of Biology Leiden, Leiden University, Sylviusweg 72, 2333 BE Leiden, the Netherlands

Abstract

The model plant *Arabidopsis thaliana* (Arabidopsis) is considered to be a monocarpic species based on commonly used early flowering ecotypes (e.g. Col-0 and Ler). For these ecotypes flowering is initiated once, followed by seed set, senescence and death of the whole plant. Polycarpic plants, on the other hand, can flower multiple times in their life cycle and maintain vegetative development during and between each flowering event. The precise mechanism with which vegetative development is regulated and restarted in polycarpic plants remains elusive. Investigating polycarpic traits, such as the formation of vegetative aerial rosettes (ARs) from inflorescence axillary meristems in Arabidopsis can improve the understanding of polycarpic development. In this study, we characterized 12 Arabidopsis ecotypes displaying polycarpic features with the formation of ARs as the main indicative phenotype. By comparing the natural variation in expression of genes known to be involved in the AR phenotype to phenotypic data, we showed that expression of *SUPPRESSOR of OVEREXPRESSION of CONSTANS 1* (*SOC1*) and *FLOWERING LOCUS C* (*FLC*) are the strongest predictors of the AR phenotype in Arabidopsis, confirming earlier findings on the role of these genes in the polycarpic life history strategy of *Arabis alpina*. In addition, we show that *AT-HOOK MOTIF NUCLEAR LOCALIZED 20* (*AHL20*) expression correlates with the AR phenotype, indicating its potential role in the polycarpic life history strategy. Finally, we show that *FLC* silencing by vernalization is sufficient to repress AR production, indicating that *FLC* acts upstream of other genes involved in AR production. Together, our data show that variation in gene expression can reliably predict phenotypic variation. This shows that correlating natural variation in polycarpic traits with natural variation in gene expression can help identify new genes involved in polycarpic development.

Keywords: life history strategy, monocarpy, polycarpy, aerial rosettes, natural variation, vernalization, *FLC, SOC1, AHL15, AHL20, SPL15*

Introduction

Flowering plants generally follow one of two life history strategies: monocarpy or polycarpy. The monocarpic life cycle includes only a single flowering period, eventually leading to a general arrest of all vegetative development and to the plant's death following seed set. During monocarpic flowering, the plant's axillary meristems (AMs) either transition to the inflorescence fate or remain dormant (Thomas, 2013). Polycarpic plants, on the other hand, can initiate flowering repeatedly and maintain vegetative development between flowering cycles (Thomas, 2013; Kiefer et al., 2019). This renewed vegetative development requires the maintenance of vegetative meristems during flowering (Amasino, 2009; Vayssières et al., 2020). Monocarps and polycarps thus regulate axillary meristem identity differently, and this difference can be clearly seen when comparing the two *Brassicaceae* species *Arabidopsis thaliana* (Arabidopsis) and *Arabis alpina.* Unlike Arabidopsis, which is considered to be monocarpic, the polycarp *A. alpina* maintains vegetative identity in part of its AMs during flowering (Ponraj and Theres, 2020; Vayssières et al., 2020). The *A. alpina* gene *PERPETUAL FLOWERING 1 (PEP1)* is a homolog of the Arabidopsis gene *FLOWERING LOCUS C (FLC),* and has been identified as a regulator of polycarpy in this species. It was shown that a renewed expression of the floral repressor *PEP1* in *A. alpina* after vernalization is sufficient to maintain a vegetative identity in axillary buds of flowering plants (Kiefer et al., 2017; Hyun et al., 2019; Tilmes et al., 2019). Therefore, FLC/PEP1 is not only important in coordinating the timing of flowering in vernalization-dependent plants, but is also involved in renewing vegetative development in *Brassicaceae* species.

In Arabidopsis, the protein FRIGIDA (FRI) acts upstream of *FLC* to promote its expression. Vernalization results in degradation of FRI and activates several other mechanisms that together cause silencing of *FLC* expression (Hu et al., 2014). The commonly studied ecotypes Col-0 and Ler carry a *fri* loss-of-function allele that causes a permanent loss of *FLC* expression, resulting in rapid flowering cycles. In contrast, most Arabidopsis ecotypes contain a functional *FRI* allele and consequently flower late when not vernalized (Johanson et al., 2000; Zhang and Jiménez-Gómez, 2020). Unlike the temporary silencing of *PEP1* in *A. alpina*, vernalization permanently silences the expression of *FLC* in Arabidopsis and in *A. alpina's* monocarpic relative *Arabis montbretiana* (Kiefer et al., 2017). The phenotype of Arabidopsis ecotype Landsberg erecta (Ler) plants overexpressing *FLC* also illustrates this: in addition to a severely delayed flowering time, these plants also produce rosette leaves from the inflorescence AMs in structures called aerial rosettes (ARs) (Wang et al., 2007).

Together, these data indicate that re-initiation of *FLC* expression in polycarpic plants is a key process allowing renewed vegetative- and therefore polycarpic development.

Since polycarpic species retain vegetative identity in some AMs, studying factors that regulate AM identity can reveal new regulators of polycarpy. Most AMs on the inflorescences of Arabidopsis ecotype Colombia-0 (Col-0) plants develop into a secondary- or tertiary inflorescence branch, indicating that they are in an inflorescence meristem (IM) state. However, some ecotypes and mutants are capable of producing ARs from these AMs, implying a more vegetative state in these AMs. The status of an inflorescence AM can therefore be deduced from the type of tissue it produces, and the production of ARs in Arabidopsis indicates a form of ectopic vegetative development. In addition to *FLC* overexpression, several other mutants with ARs have been identified, which has shed light on other potential regulators of polycarpic development. For example, loss-of-function of both MADS-box genes *SUPPRESSOR of OVEREXPRESSION of CONSTANS 1* (*SOC1*) and *FRUITFULL* (*FUL*) causes delayed flowering and ectopic vegetative growth in the form of ARs (Melzer et al., 2008). Individually, loss-of-function of *soc1* causes a strong delay in flowering time and increased bract formation in inflorescences, whereas the *ful* mutation reduces fruit size and inflorescence determinacy and only shows a mild increase in flowering time (Melzer et al., 2008; Dorca-Fornell et al., 2011; Balanzà et al., 2014). SOC1 and FUL interact *in vivo* to regulate expression of their target genes, and the *soc1 ful* double mutant shows a strongly delayed flowering time, enhanced vegetative growth, longer life span, and multiple flowering cycles, indicating that these genes repress vegetative development and polycarpic growth (Melzer et al., 2008). In addition, knockout of several members of the adult-phase *SQUAMOSA PROMOTER-LIKE (SPL)* transcription factor gene family also delays the juvenile-to-adult transition known as vegetative phase change (VPC) and causes delayed flowering and AR production. This is similar to phenotypes observed in lines overexpressing the juvenile-phase microRNA *miR156* that regulates mRNA abundance of several *SPL* genes (Wu and Poethig, 2006; Schwarz et al., 2008). The similarity in phenotypes between the *soc1 ful*, *spl,* and *p35S:MIR156* mutants can be partially explained by the fact that SOC1 and SPL15 co-regulate the expression of some genes (Hyun et al., 2016). In addition, *SOC1* and *SPL15* are repressed by FLC (Deng et al., 2011), and SPL15 is required for vernalization-induced flowering in *A. alpina*, as only plants that are vernalized after a certain age can initiate flowering when returned to ambient temperatures (Hyun et al., 2019).

Recently, we identified the *AT-HOOK MOTIF NUCLEAR LOCALISED 15 (AHL15)* gene as another key switch between mono- and polycarpic life history strategy in Arabidopsis. Plants overexpressing *AHL15* show a similar AR-producing phenotype as the aforementioned *soc1 ful* or *spl* mutants or the *MIR156* overexpression lines (Karami et al., 2020; Rahimi et al., 2022). Moreover, *ahl15* loss-of-function almost completely abolishes the polycarpic AR-phenotype of the *soc1 ful* mutant, and ChIP-qPCR and EMSA experiments showed that SOC1 and FUL bind regions up- and downstream of the *AHL15* gene (Karami et al., 2020). In addition, we observed reciprocal negative feedback between *AHL15* and *SPL* genes (Rahimi et al., 2022). These results indicate that AHL15 delays AM maturation, thereby maintaining their vegetative state by repressing components of the ageing pathway. However, in wild-type Arabidopsis, *AHL15* expression is repressed by the SOC1/FUL-triggered flowering and SPL-mediated ageing pathways, resulting in a monocarpic life history strategy. Interestingly, *AHL15* and its close homologs *AHL19* and *AHL20* are upregulated after flowering in the polycarpic *Arabidopsis lyrata* but not in Arabidopsis, indicating that these genes could be involved in the polycarpic life history strategy of this species (Karami et al., 2020).

In this study, we identified and analysed 12 Arabidopsis ecotypes that show the AR phenotype and other polycarpic traits, and compared their development to Col-0. All selected ecotypes show delayed flowering, but neither this nor the AR phenotype correlate with a prolonged juvenile phase. We show that FLC is responsible for the AR phenotype of these ecotypes, but is not the sole factor explaining AR production. We provide further evidence that expression of *SOC1* and *SPL15* is negatively correlated to the production of ARs in different genetic backgrounds, and that in addition to *FLC*, expression of the *AHL15* homolog *AHL20* positively correlates with AR production. Moreover, co-expression analyses imply that expression of *FLC* and *AHL15* and of *SOC1* and *AHL20* are linked, which reveals potential new interactions within regulatory pathways. In conclusion, our data shows that variation in gene expression can be reliably linked to variations in polycarpic traits in wild-type Arabidopsis plants.

Results

Phenotypes of AR-producing ecotypes

In this study, we used an unbiased approach to look at which key regulators determine natural variation in polycarpic traits in Arabidopsis, with the AR phenotype as key trait. Because most research on the AR phenotype has been

based either on studying Arabidopsis mutants or on the description of a single ecotype, we set out to study the AR phenotype in non-mutant conditions in a larger set of ecotypes. To do this, we searched for ecotypes producing ARs based on their phenotypic description in the NASC database, and selected twelve ecotypes based on their phenotype and availability. These twelve ecotypes originate from different environments and a large geographical range in terms of latitude and longitude, ensuring diversity in genetic background as well as environmental adaptations (Supplementary figure 1).

To compare the phenotypes of the AR ecotypes in an unbiased manner, we scored a number of polycarpy-related phenotypes at five weeks after bolting for each ecotype. First, the total number of ARs on all inflorescences was counted at five weeks after bolting for each ecotype and compared to the total number of inflorescence AMs (IAMs) to calculate the percentage ARs (Figure 1A, B). The latter number was used to rank the ecotypes according to their AR production phenotype. The ecotypes were left to continue growing in the same climate room for up to six months to monitor the phenotype at later stages (Supplementary figure 2).The percentage of IAMs producing ARs differed strongly between ecotypes, with Es-0 producing ARs in over 40% of the inflorescence AMs, while other ecotypes like Tha-1, Mv-0 and Gifu-2 only produced very few ARs at this time point (Figure 1A, B). The timing of ARs emergence also differed between ecotypes: in some, like Es-0, Kas-2, and Had-1B, ARs could be observed as early as three weeks after bolting, whereas in other ecotypes such as Mv-0 and Gifu-2 no ARs were produced until after the five-week time point (Supplementary figures 2 and 3E-M). During pilot experiments, we observed that the first (lowest) IAM on the primary inflorescence was usually the first to produce an AR, which also developed the most rosette-like leaves of all ARs on the inflorescence. We counted the number of leaves produced from this IAM on the first node (Figure 1C), to test if this could be an early indicator for the overall AR production, as measured by the percentage of IAMs forming ARs (Figure 1A). Although the ranking between the two methods did not match perfectly, Es-0 came out as the ecotype with the strongest AR phenotype in both methods, and ecotypes that produced few ARs (such as Tha-1, Do-0, and Hh-0) still had a higher number of leaves at the first IAM than Col-0 (Figure 1C). At six months after sowing, all ecotypes except Col-0, which had completely senesced by this time, produced ARs in varying quantities and continued to grow, producing more ARs (Supplementary Figure 2). This indicated that in these AR-producing ecotypes, like in polycarpic species, not all IAMs become reproductive upon flowering and that as a result flowering does not trigger

whole-plant senescence.

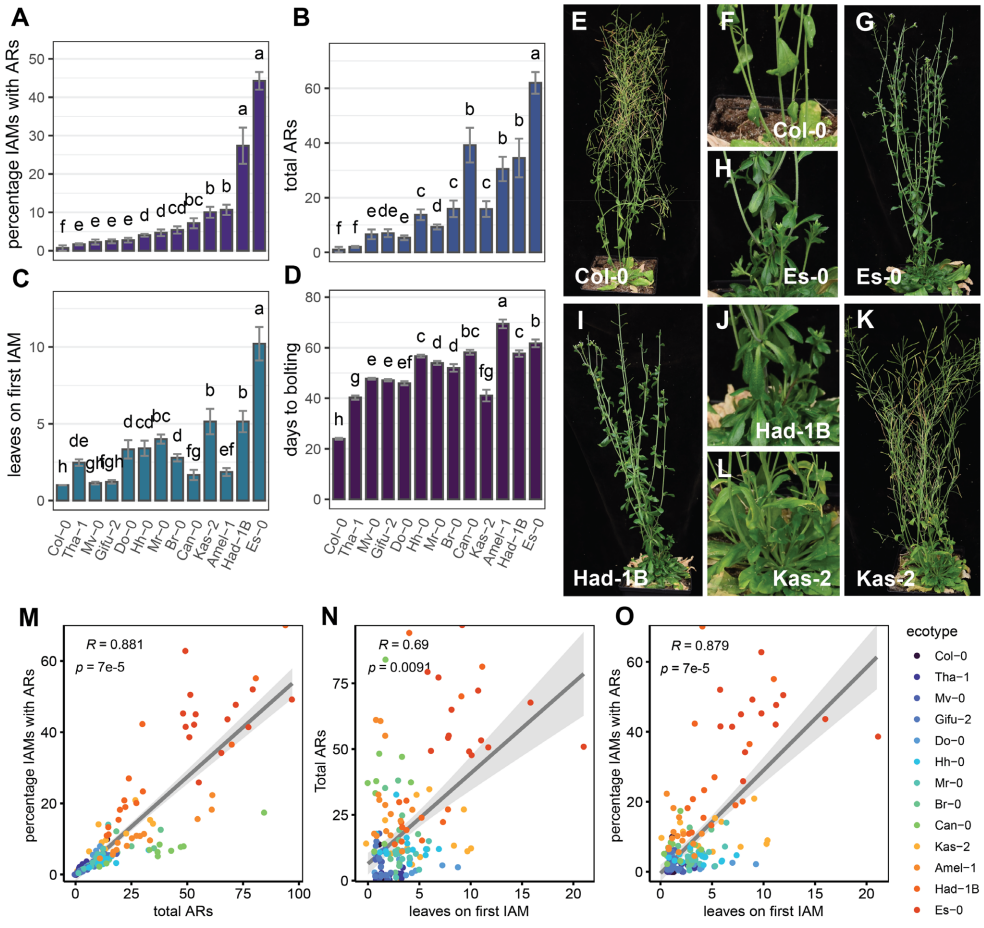

Figure 1: Phenotypes of AR-producing Arabidopsis ecotypes grown in lovng day conditions at five weeks after bolting. **A**: The percentage of inflorescence axillary meristems (IAMs) bearing three of more leaves. **B**: The total number of IAMs bearing three or more leaves. **C:** The number of leaves on the first AM of the primary inflorescence. **D:** Number of days from the start of seed germination to the first visible bolt. For each ecotype in figures **A-D**, 10-15 plants were analyzed and groups were compared with the Kruskall-Wallis test. Letters above bars indicate significance groups; different letters indicate significant differences between measurements. **E-L:** Phenotype of three of the AR-producing ecotypes compared to Col-0 at five weeks after bolting. All pots are 11 cm wide. **M:** Correlation of the total number of ARs with the percentage of IAMs bearing ARs. **N:** Correlation of the total number of ARs with the number of leaves produced by the first IAM. **O:** Correlation between the percentage of IAMs bearing ARs and the number of leaves produced by the first IAM. Correlation analyses in **M-O** were performed using Pearson's correlation, data are based on 10-15 plants per ecotype with a total of 172 plants.

The bolting time varied among ecotypes, but was significantly delayed for all ecotypes compared to Col-0 (Figure 1D). In order to exclude the possibility

that the AR phenotype was caused by delayed vegetative phase change (VPC), we counted the number of leaves lacking abaxial trichomes as a measure of juvenility (Supplementary figure 4A). We did not compare the length : width ratio of leaves between ecotypes, as the leaf shape varied strongly between ecotypes, making it an unreliable VPC marker. For some ecotypes, such as Es-0, both a delayed bolting time and a prolonged juvenile phase were observed, but generally there was no clear correlation between length of the juvenile phase and bolting time or the total number of ARs (Supplementary figure 4B, C). In fact, in several AR ecotypes VPC occurred significantly earlier than in Col-0.

Linear regression analysis (Pearson's correlation, n = 172) showed that the percentage of ARs strongly correlated with the total number of ARs (Figure 1M). Both the total number of ARs and the percentage of ARs also correlated positively with the number of leaves on the first IAM (Figure 1N and 1O). This shows that the number of leaves on the first IAM could be a sufficiently accurate measure to assess the AR trait in a more high-throughput manner than by counting all the IAMs with and without ARs. Finally, bolting time correlated significantly with all other polycarpic phenotypes (Supplementary figure 5), suggesting that at least in Arabidopsis, polycarpy coincides with late flowering.

Expression of polycarpy-related genes in AR-producing ecotypes

In previous research, ARs have been observed in different mutant or overexpression lines in which the floral transition was affected. The mutated or overexpressed genes are known to act in a regulatory network with the vernalization-repressed gene *FLC*, which represses the expression of *SOC1* and *SPL* genes (Figure 2A). SOC1 inhibits AR formation by repressing the expression of *AHL15* (Karami et al., 2020), and *AHL15* and several *SPL* genes interact in a reciprocal negative feedback loop (Rahimi et al., 2022). To understand whether the AR phenotype in AR ecotypes is caused by differential expression of one or more of the genes in this network, we performed RT-qPCR on RNA isolated from plant tissues at three different phases of development, i.e. in juvenile plants, in the rosette base at bolting (RBB), and in the IAMs at five weeks after bolting.

AHL15 expression was similar for all ecotypes at the juvenile stage, and generally increased in the RBB for AR ecotypes but not Col-0, and decreased again in the IAMs (Supplementary figure 6A-C, G). *AHL20* expression followed a similar pattern, and was strongly enhanced in the RBB for most AR ecotypes compared to Col-0 (Supplementary figure 6D-F, H). *AHL19* could barely be detected in all ecotypes during the juvenile stage nor in the RBB, and was

therefore excluded from the analysis. The expression of *FLC* was higher in all AR ecotypes compared to Col-0 at all stages (Supplementary figure 6G-H). This enhanced *FLC* expression explains the delayed bolting time of the ecotypes, and could also explain the observed AR phenotype.

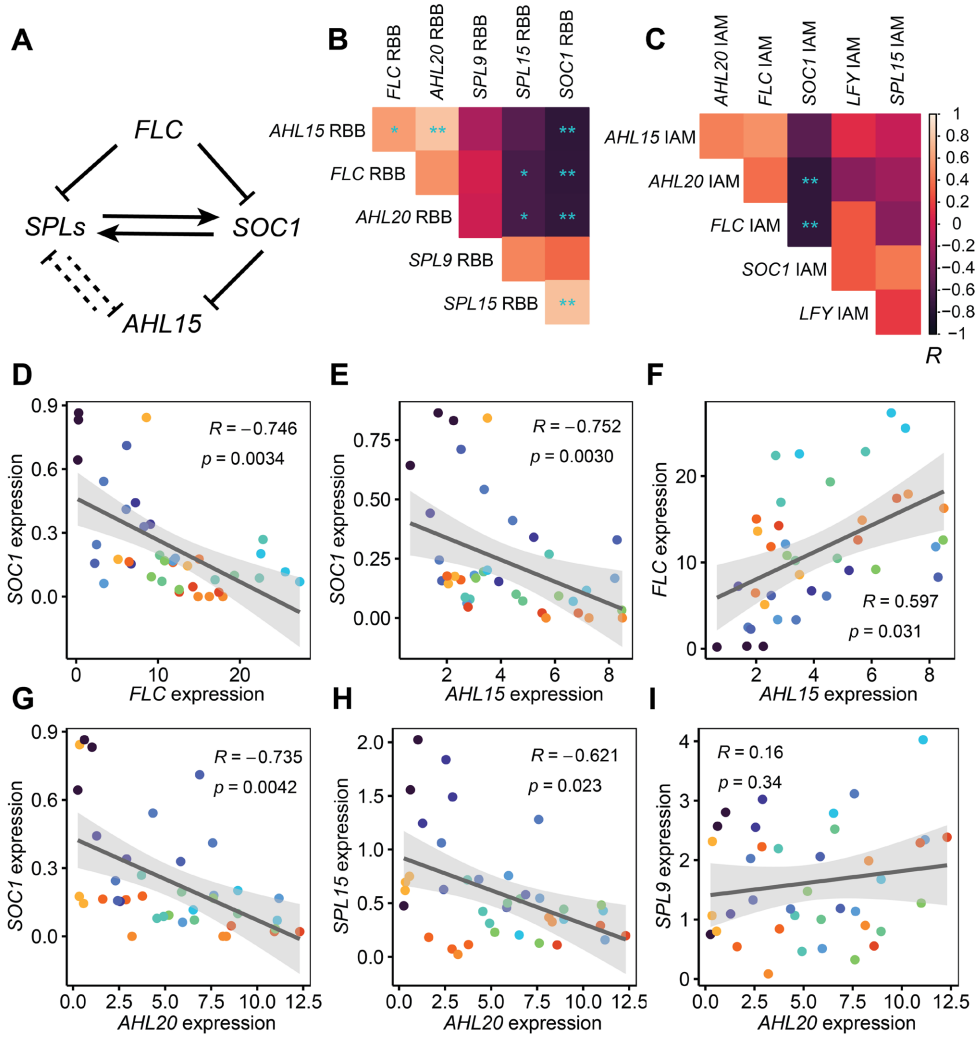

Figure 2: Correlations between expression of genes in AR ecotypes. **A:** Interaction network between *FLC*, *SOC1*, *SPL* and *AHL15* genes based on literature. **B:** Heatmap showing Pearson's correlation between genes expressed in the rosette base at bolting (RBB). **C:** Heatmap showing Pearson's correlation between genes expressed in the inflorescence axillary meristem (IAM) at five weeks after bolting. Blue stars indicate statistically significant correlations (*: p<0.05, **: p<0.01, ***: p<0.001), and tile colors are scaled to the Pearson's R coefficient. **D-I:** Examples of individual Pearson's correlations between genes expressed in the RBB. For each correlation analysis, 36 samples from 13 ecotypes were included.

In contrast, the expression of *SOC1* in the RBB was significantly lower than in Col-0 for most AR ecotypes, and its expression increased in the IAMs where the differences between ecotypes were less pronounced (Supplementary figure 7A-C). *SPL9* expression was similar for all ecotypes in the RBB (Supplementary figure 7E), while *SPL15* expression appeared reduced in most AR ecotypes in both the RBB and IAMs, but not significantly (Supplementary figure 7C, D).

In order to establish whether the AR-producing IAMs were in a vegetative or reproductive state, we studied the expression of the floral meristem identity gene *LEAFY (LFY)* (Weigel and Nilsson, 1995). Surprisingly, *LFY* expression in the IAMs was similar to Col-0 in most ecotypes (Supplementary figure 7F). This indicates that the IAMs maintain a floral identity despite producing vegetative structures, which is illustrated by the fact that from some ARs, a secondary or tertiary inflorescence can still emerge (Figure 1H-K, Supplementary figure 3E-M).

In summary, *FLC* and *SOC1* expression showed a clear difference in expression between the AR ecotypes and Col-0. However, due to the high variation between biological triplicates it was difficult to conclude on the role of *AHL* and *SPL* genes in the AR phenotype. We therefore decided to perform a more global analysis of the interaction between the genes that were measured in the RBB and IAM tissues.

With the expression data from the RBB and IAM tissues, we investigated the interaction between genes by linear regression (Pearson's correlation, Figure 2, Supplementary table 1). By adding the biological replicates of each ecotype in the analysis individually, we reduced the weight of "genotype" as a factor in the analysis. As expected*, FLC* and *SOC1* showed a significant negative correlation in both tissues (Figure 2B-D). *SOC1* expression also correlated negatively with *AHL15* in the RBB (Figure 2B, 2E), confirming earlier reports that *AHL15* expression is repressed by SOC1 (Karami et al., 2020). Interestingly, *SOC1* and *AHL20* expression also negatively correlated in the RBB and the IAMs (Figure 2B, C, G), indicating that both *AHL15* and *AHL20* might play similar roles downstream of SOC1. In line with this, *AHL15* and *AHL20* expression showed a significant positive correlation in the RBB (Figure 2B). *FLC* expression correlated positively with *AHL15* but not with *AHL20* expression, and negatively with *SPL15* expression in the RBB (Figure 2B, F). Finally, we tested whether there was a correlation between the expression of the *AHL* and *SPL* genes in this experiment. Surprisingly, a significant negative correlation could be seen between expression of *SPL15* and *AHL20,* but not *AHL15* in the RBB (Figure 2B, H)*. SPL9* and *LFY* expression did not correlate positively or negatively to the

expression of any of the genes tested (Figure 2B, C, I).

Together, the expression patterns of these *TF* genes in different ecotypes and the correlations found between these genes confirm gene interaction networks identified in earlier studies based on mutant screens in the Col-0 or Ler background (Figure 2A). Our results show that by comparing expression data collected from a panel of ecotypes, the same interactions can be observed, but also unknown interactions between genes are revealed (e.g. between *SOC1*, *SPL15* and *AHL20*).

Expression of *FLC, AHL20* and *SOC1* predicts AR production

Because the ecotypes showed variation in phenotype as well as in gene expression, we investigated whether gene expression correlated with the observed phenotypes and whether it could be a good predictor of the phenotype. The average gene expression in the IAMs (collected directly after phenotyping at five weeks after bolting) and expression in the RBB (collected in an independent experiment in the same growth chamber) were both compared to the average bolting time and the AR traits measured at five weeks after bolting (Figure 3, Supplementary table 1).

AHL15, AHL20, and FLC have each been shown to delay flowering time in Col-0 (Gu et al., 2013; Karami et al., 2020; Tayengwa et al., 2020). From our data, there is a clear positive correlation between bolting time and *AHL15*, *AHL20*, and *FLC* expression, indicating that these genes play similar roles in our panel of ecotypes (Figure 3A). We also observed a strong negative correlation between bolting time and *SOC1* expression in both tissues (Figure 3A), again showing that expression data can predict interactions between genes and their associated phenotypes.

Next, we looked at the interaction between gene expression and the AR phenotype. As expected, we could see a significant negative correlation between *SOC1* expression in both tissues and the total number of ARs (Figure 3A, D). The total number of ARs was also negatively influenced by *SPL15* expression in the RBB, but surprisingly not in IAMs (Figure 3A). *FLC* expression in the IAMs correlated positively with all three indicators of AR production (Figure 3A-C). Surprisingly, we also observed a significant positive correlation between *AHL20* expression and the total number of ARs, but not for *AHL15* (Figure 3A, E). This suggests that AHL20 might play a similar, if not more important role than AHL15 in AR production downstream of SOC1 in the tested AR ecotypes.

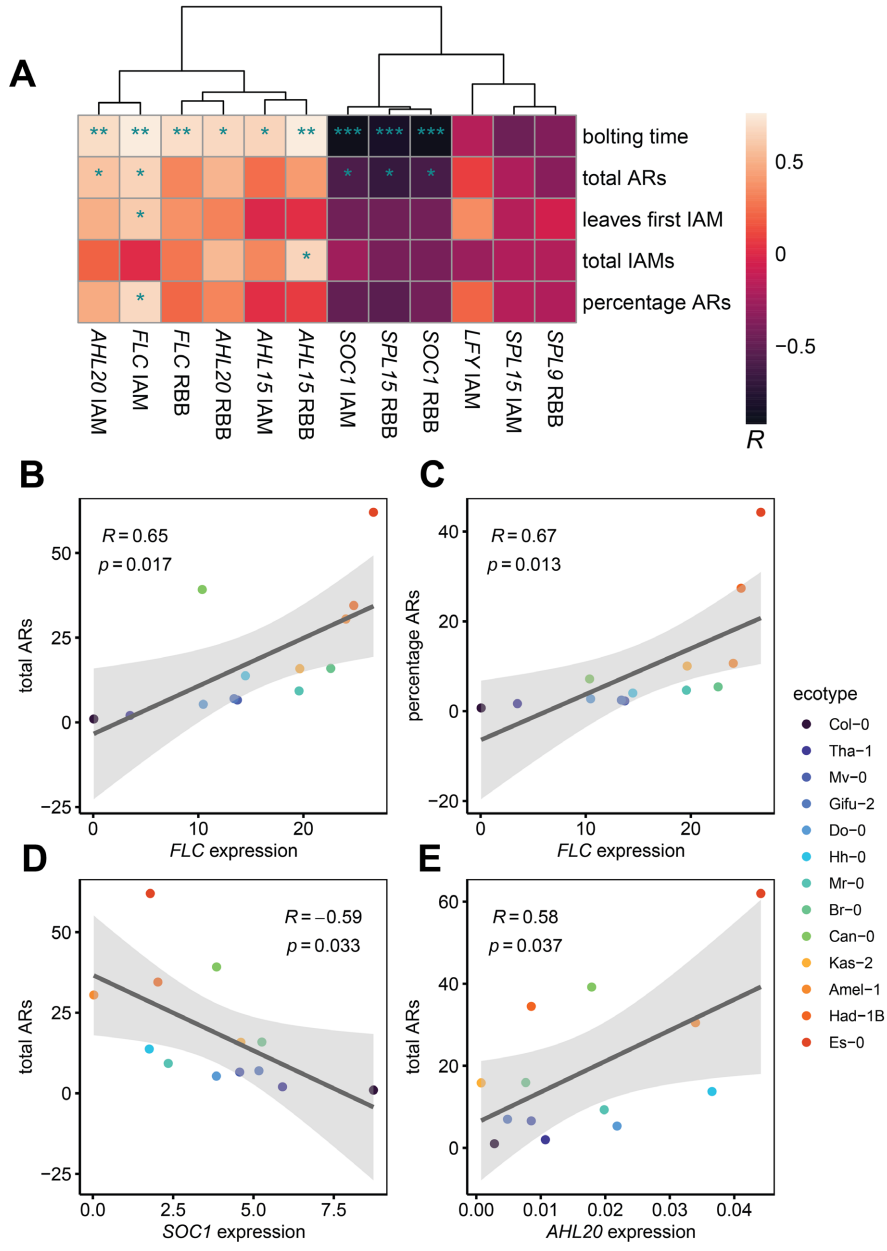

Principal component analysis of phenotypic- and gene expression data reveals SOC1 as the major driver of diversity

Because the expression of multiple genes correlates significantly with the AR phenotype, we performed a principal component analysis (PCA) to identify the gene that most strongly influences the variation between ecotypes. We

Figure 3 (left page): Correlations between expression of genes and the AR phenotype at five weeks after bolting. **A:** Heatmap showing Pearson's correlation analysis between phenotypic data and expression of genes in the rosette base at bolting (RBB) or in the inflorescence axillary meristem (IAM) at five weeks after bolting. Blue stars indicate statistically significant correlations (*: p<0.05, **: p<0.01, ***: p<0.001), and tile colors are according to the indicated Pearson's R coefficient color scale. **B-C:** Pearson's correlation analysis of *FLC* expression in the IAMs with the total number of ARs (**B**) or the percentage of ARs (**C**). **D-E:** Pearson's correlation analysis of the total number of ARs and the expression of *SOC1* (**D**) or *AHL20* in the IAMs (**E**). Mean values of gene expression of 2-3 biological replicates consisting of material from three plants each and phenotypic traits of 10-15 plants per ecotype were used for the analysis.

compared average gene expression at both stages (in the RBB and in IAMs) between all ecotypes, and found that the strongest driver of variation between ecotypes is the expression of *SOC1* in both the RBB and IAM, followed by expression of *AHL15* and *FLC* in the RBB (Figure 4, Supplementary table 2A). This is represented by their respective contribution to the first principal component (PC1) in the PCA, which is highest for *SOC1* expression in the RBB followed by *SOC1* expression in the IAM (Supplementary table 2A). In addition, *SOC1* expression showed the strongest (negative) correlation with the AR phenotype of all genes (Figure 3A, D) and the importance of *SOC1* for the AR phenotype is further confirmed by its strong contribution to PC1. Furthermore, this PCA shows that the expression of genes in the RBB varies more strongly between ecotypes and has a stronger influence on variation between ecotypes. This could indicate that gene expression during the bolting phase might be more indicative of the later shoot phenotype than gene expression at later developmental stages. The observed correlation of the AR phenotype with *SPL15* expression in the RBB, but not in IAMs further supports this (Figure 3A).

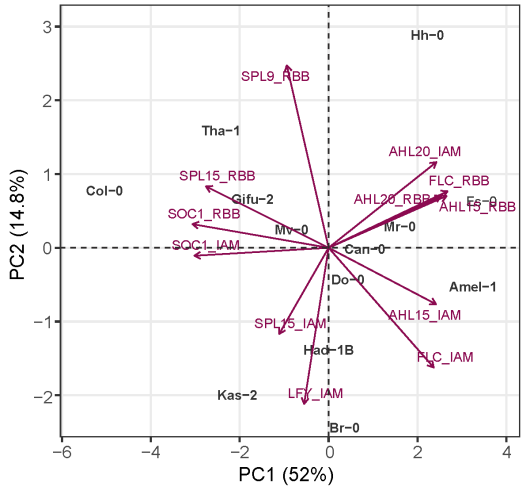

Figure 4: Principal component analysis of variation between ecotypes based on gene expression in rosette before bolting (RBB) or inflorescence axillary meristems (IAM) tissue. The length and direction of the arrows (in purple) indicate the weight with which the variable contributes to the first two principal components. Ecotype names (in black) are plotted based on the first two principal components. Mean values for gene expression of 2-3 biological replicates consisting of material from three plants each were used for the analysis.

FLC is required for aerial rosette production

Because of the significant positive correlation between *FLC* expression and AR production, we tested whether the ecotypes would still produce ARs when *FLC* was no longer expressed. In order to do this, we measured the same phenotypic traits in plants that had been subjected to a five-week seed vernalization treatment, which should be sufficient time for silencing of *FLC* in most ecotypes (Duncan et al., 2015).

Vernalization treatment strongly accelerated bolting time in all ecotypes, except for Had-1B and Mr-0, which flowered only slightly earlier than in non-vernalized control conditions (Figure 5A). At five weeks after bolting, the phenotype of vernalized plants was markedly different from their non-vernalized counterparts (Figure 5D-H, Figure 1E-K, Supplementary figures 3, 9). First, most vernalized ecotypes no longer produced ARs at five weeks after bolting, except Had-1B and Mr-0, which were also the latest to bolt (Figure 5A, B). Second, in many cases the leaf- and inflorescence morphology of vernalized plants was markedly different compared to their non-vernalized counterparts. This was especially obvious in ecotypes Es-0, Kas-2 and Amel-1 (Figure 5D, E, H). Non-vernalized Es-0 plants, for example, had dark-green leaves with a firm texture and prominent trichomes in control conditions, whereas the colour and texture of the leaves became lighter and less rigid following vernalization.

In order to confirm whether the absence of ARs was indeed a result of decreased *FLC* expression, the expression of *FLC* was analysed in the IAMs of the two ecotypes still producing ARs (Had-1B and Mr-0) as well as three ecotypes producing the highest percentage of IAMs (Es-0, Amel-1, Kas-2) (Figure 5C). *FLC* expression was significantly reduced in Kas-2, Amel-1 and Es-0, while its expression remained high in Had-1B and Mr-0. The continued expression of *FLC* in the latter two ecotypes explains the late bolting time and continued production of ARs, and suggests that the vernalization period was too short for full *FLC* repression in these ecotypes. The absence of ARs and the repressed expression of *FLC* in the three other vernalized AR ecotypes, along with the strong and significant positive correlation between *FLC* expression and AR production in non-vernalized plants show that *FLC* is the main determinant of AR production in these ecotypes. *FLC* is likely to act upstream of *SOC1, SPL15,* and *AHL20*, whose expression was shown to correlate with the total number of ARs in this study.

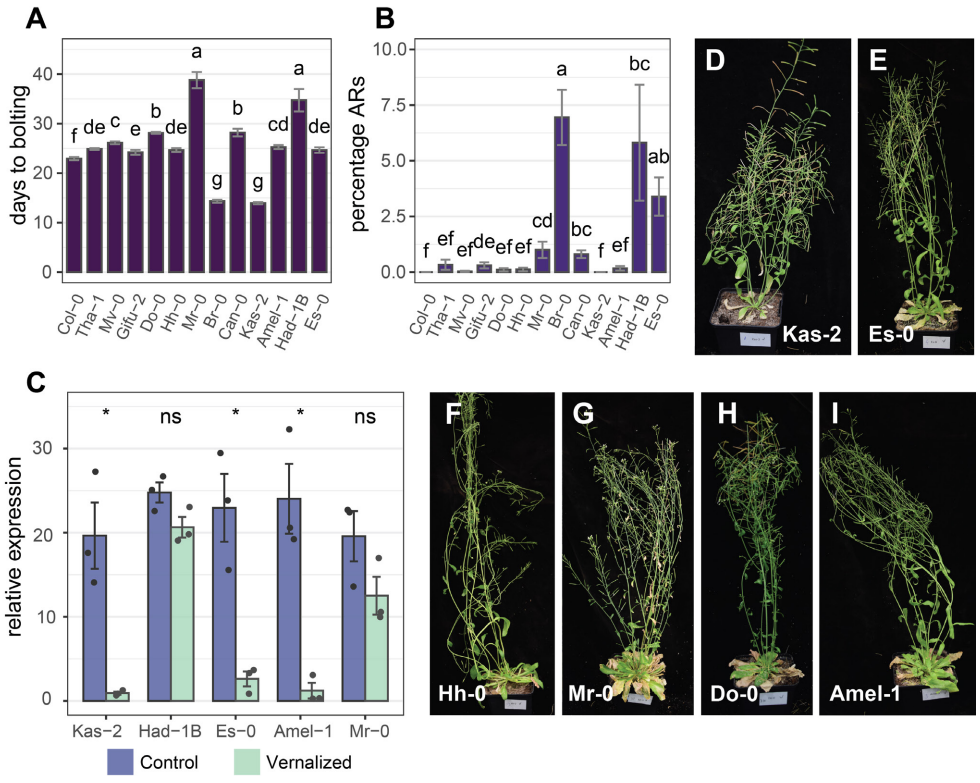

Figure 5: Phenotypes of vernalized AR ecotypes at five weeks after bolting. **A:** Days between the end of seed vernalization and the first visible bolt. **B:** The percentage of IAMs bearing three or more rosette leaves. For each ecotype in **A** and **B**, 15 plants were analyzed, and groups were compared with the Kruskall-Wallis test. Statistically significant differences are indicated with different letters above the bars. **C:** Expression of *FLC* in IAMs at five weeks after bolting in non-vernalized (blue) and vernalized plants (turquoise). Each measurement is based on three biological repeats, and differences between non-vernalized and vernalized were compared using a Student's *t*-test. Asterisk indicates a significant difference ($p < 0.05$) ; ns = not significant. **D-H**: phenotypes of vernalized plants of the indicated ecotypes at five weeks after bolting. All pots are 9 cm wide.

Discussion

In Arabidopsis, the AR phenotype can be observed in mutants in which the flowering pathway is affected or repressed (Wang et al., 2007; Melzer et al., 2008; Xu et al., 2016; Karami et al., 2020). In this research, we have studied multiple Arabidopsis accessions that naturally produce ARs and investigated the relationship between the AR phenotype and the expression of genes that have previously been shown to affect AR production. Our results show that the floral repressor *FLC* is the major determinant of AR production in this panel of accessions, and that silencing *FLC* expression by vernalization is sufficient to

repress the AR phenotype. In addition, we show that the expression of *SOC1* in both early- and late stages of flowering is negatively associated with the AR phenotype. Our findings confirm earlier results that show that knockout of *soc1* in combination with *ful,* or overexpression of *FLC* results in an AR-producing phenotype, similar to that seen in the strongest AR ecotypes such as Es-0. This shows that gene function can be deduced by correlating gene expression to phenotypic traits when studying a panel of phenotypically diverse genotypes, avoiding the need for using transgenic- or mutagenized lines. In addition, we have shown that this method can identify interactions between genes based on their expression, as can be seen for the negative correlation between the expression of *SOC1* and its repressor *FLC*.

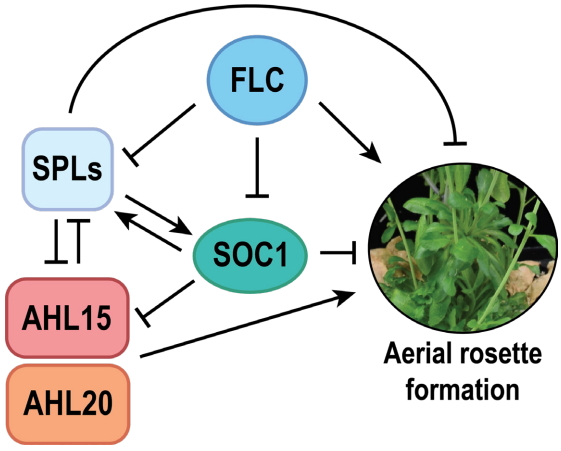

Figure 6: Genetic regulation of aerial rosette formation. SOC1 and SPL15 repress the formation of ARs, whereas FLC, AHL15, and AHL20 promote the formation of ARs. FLC represses expression of *SOC1* and *SPL15*, and its expression correlates positively with *AHL15* expression. SOC1 represses expression of *AHL15* and *AHL20*, and promotes *SPL15* expression and *vice versa*.

AHL20 as a new player in AR production

Our data show that expression of the *AT-HOOK MOTIF NUCLEAR LOCALISED* family gene *AHL20* in the IAMs positively correlates with AR formation, and that it is likely repressed by SOC1, identifying a previously unknown function for this gene (Figure 6). Surprisingly, despite previous evidence that *AHL15* is required for the AR phenotype in the *soc1ful* mutant and is directly repressed by SOC1 in the IAMs (Karami et al., 2020), the expression of *AHL15* in the IAMs did not show a significant correlation with the AR phenotype. RNA-seq data shows that both *AHL15* and *AHL20* are upregulated in the stem of the *soc1ful* mutant, indicating that *AHL20* could be another direct target of SOC1 (Davin et al., 2016). However, ChIP-seq on the shoot apices of short day (SD)-grown *gSOC1:GFP* plants showed significant enrichment at the *AHL15* locus, but not the *AHL20* locus (Immink et al., 2012), which suggests that *AHL20* is

not directly repressed by SOC1, or possibly that SOC1 targets differ between SD and (in our case) LD-grown plants and between shoot apices and stem tissue. The RBB samples were enriched in stem tissue, and we found a strongly enhanced *AHL20* expression in the AR ecotypes compared to Col-0 in these samples. It is therefore possible that *AHL20* has an expanded function during the floral transition or in stem tissue in the AR ecotypes, or is targeted by SOC1 specifically in this tissue type.

Interestingly, *AHL20* expression in the IAMs was much lower than that of *AHL15,* but was a better predictor of AR production. Previous studies on *AHL* genes have revealed a high level of functional redundancy (Zhao et al., 2013; Karami et al., 2020; Rahimi et al., 2022), and it is likely that *AHL20* and *AHL15* play very similar roles in promoting vegetative development of AMs. Considering the number of genes associated with the AR phenotype in Arabidopsis, it is likely that in addition to *AHL15* and *AHL20*, the production of ARs is controlled by other factors that act downstream of FLC, SOC1, and SPL15, such as the NAC TF ANAC087 (Vargas-Hernández et al., 2022), and RADICAL-INDUCED CELL DEATH 1 (RCD1) and SIMILAR TO RCD-ONE1 (SRO1) (Teotia and Lamb, 2009). *AHL* genes might therefore also play a more nuanced role in wild-type plants than when overexpressed, a situation where the high dose of AHLs might override the balanced regulation of AM outgrowth. Taken together, our data clearly show that FLC and AHL20 promote AR formation whereas SPL15 and especially SOC1 repress AR formation (Figure 6).

FLC is a major determinant of AR production

Previous research has shown that an altered *FLC* expression resulting from changes in its upstream regulator AERIAL ROSETTE 1 (ART1)/HUA2 was responsible for the AR phenotype in the Arabidopsis ecotype Sy-0 (Wang et al., 2007). Unfortunately, the authors did not investigate whether the AR phenotype persisted after vernalization, which would indicate whether any other factors are responsible for AR formation in this ecotype. Here, we show that *FLC* plays a similar role in ecotypes retrieved from geographically diverse locations, indicating that this mechanism is conserved.

FLC has been shown to be required for the polycarpic life history strategy in *Arabis alpina* by protecting AMs from transitioning into an inflorescence- or floral identity (Hyun et al., 2019; Kiefer et al., 2019). *A. alpina* starts flowering when *FLC* /*PEP1* expression is temporarily repressed by vernalization, but re-initiates vegetative growth due to a reset of *FLC/PEP1* expression. Our data show that FLC can play a similar role in the monocarpic Arabidopsis in

the absence of vernalization, and causes a significant increase in life span when its expression remains high during flowering. It has been shown that *FLC* expression is regulated differently between monocarps like *Arabis montbretiana* and Arabidopsis compared to the polycarpic *A. alpina*, and that this is a result of sequence variation in the regulatory elements of the *FLC* locus (Kiefer et al., 2017). A recent study has shown that similar differences in *FLC* regulation are key to the differences in the life history strategy of two other *Brassicaceae* genera (Zhai et al., 2024). These studies make it clear that FLC is a major player in the polycarpic life history strategy. However, the role of FLC in this process may be unique to the *Brassicaceae*, as it has been shown that the vernalization response is conferred by *Terminal Flower 1*-like genes in the *Rosaceae* (Kurokura et al., 2013). In addition, many polycarpic species grow in climates in which they are never exposed to vernalizing conditions. It would therefore be interesting to investigate how polycarpic development is regulated in (tropical) polycarpic species that do not experience winter cold in order to better understand the evolution of polycarpy.

SOC1 and *SPL15* have been shown to act downstream of FLC (Deng et al. 2011), and our data show that *AHL20* most likely acts downstream of SOC1 (Figure 6). It is therefore likely that FLC induces the AR phenotype by regulating the expression of these and potential other genes directly and indirectly. FLC expression alone is unlikely to be sufficient to initiate the AR phenotype, as the AR phenotype is relatively rare in Arabidopsis ecotypes, despite the fact that many ecotypes are vernalization-dependent and therefore also express *FLC* (Zhang and Jiménez-Gómez 2020). This is most likely due to differences in *FLC* expression levels similar to what we have observed in our panel of ecotypes. However, since the initiation of AR production was relatively slow in some of the ecotypes described here, it is also possible that many more vernalization-dependent ecotypes are capable of producing ARs, but have never been described as such due to the late emergence of this trait. The differences in the number of ARs and the number of leaves on the first node also shows that there is variation in the intensity of the AR phenotype, which could depend on differences in downstream target regulation. Most genome-wide association studies (GWAS) have studied pre-flowering traits or traits that can be observed soon after flowering, while longevity and life span has never been studied in much depth (Togninalli et al. 2018; Atwell et al. 2010). Studying the AR phenotype and overall life span in a larger panel of ecotypes could therefore help identify potential novel regulators of AM outgrowth and polycarpy.

Gene expression at bolting determines the inflorescence phenotype

The expression of *SOC1* and *SPL15* in RBB tissue, and *SOC1* in IAMs show a significant negative correlation with the total number of ARs. In addition, PCA shows that *SOC1* expression in both RBB and IAM tissue is the strongest driver of variation between the ecotypes in this study. These results confirm earlier studies that have shown that the FLC-repressed gene *SOC1* acts as a repressor of AR formation, as the *soc1ful* mutations in the Col-0 background produce ARs (Melzer et al. 2008; Karami et al. 2020). Similarly, the expression of *SPL15* in the RBB is negatively correlated to both *FLC* expression and the AR phenotype, and has previously been shown to repress AR formation in the Col-0 background (Rahimi et al. 2022). Our results show that these genes fulfil similar roles in geographically diverse ecotypes in repressing the outgrowth of IAMs into ARs. Although the AR phenotype often appeared only several weeks after flowering, the intensity of this phenotype in some cases correlated more strongly with gene expression in the RBB compared to expression in the IAMs (Figure 3). This observation is further supported by the PCA, which showed that five out of six of the main contributors to the first principle component were expressed during the bolting stage (Figure 4). These results suggest that the inflorescence architecture is likely to be determined before outgrowth of the inflorescence stem and rosette branches, and that gene expression at this stage can predict the inflorescence architecture.

Arabidopsis ecotypes as a tool for studying polycarpy

In this study, we have described ecotypes that display a range of polycarpic traits that include a longer life span and delayed bolting time, and most importantly the production of ARs. The renewed vegetative growth in the form of ARs on the inflorescence stems of these ecotypes resembles that of polycarpic species, showing that polycarpic traits can arise in monocarpic species. Studying polycarpic traits in species that are generally considered monocarpic can help shed light on how meristematic fate is regulated in plants with different life history strategies, and on how these differences in life history strategy have evolved. The fast life cycle and expansive genetic toolkit associated with Arabidopsis make this species a useful tool for studying such phenotypes, as even slow-flowering ecotypes, such as those described in this study, still have a relatively quicker development than other, polycarpic, species. As the formation of ARs and other post-bolting traits have been poorly covered in GWAS, focusing mainly on the plant's life span (Atwell et al. 2010),

the mechanisms driving post-bolting shoot development and longevity remain elusive. With this panel of ecotypes we show that significant variation exists even within a relatively rare trait such as AR formation, and that this trait could be an interesting subject for future GWAS. To our knowledge, this study is the first in which AR traits have been investigated in a quantitative manner, and our results show that instead of the total number and percentage of ARs, which can only be scored relatively late during development, the number of leaves on the first inflorescence node can be used as a much earlier phenotype to compare polycarpic development between ecotypes.

Methods

Plant material and growth conditions

The Arabidopsis ecotypes Amel-1 (N76434), Br-0 (N76455), Can-0 (N76109), Do-0 (N76474), Es-0 (N76484), Gifu-2 (N76494), Had-1B (N76509), Hh-0 (N76512), Kas-2 (N78905), Mv-0 (N76556), Mr-0 (N78474), Tha-1 (N76611) were acquired from the Nottingham Arabidopsis Stock Centre (NASC; www.arabidopsis.info). The Col-0 ecotype was used as a non-AR producing control.

Seeds were sown on soil (90% turf soil with 10% sand) and stratified on damp soil for 5 days at 4°C for the control conditions, or kept at 4°C in the dark for 5 weeks for seed vernalization. After stratification or seed vernalization, pots were transferred to a climate chamber and seeds were germinated under long day (16h photoperiod) at 21°C and 65% relative humidity. One week after sowing, individual seedlings were transferred to large individual pots.

The number of juvenile leaves (without abaxial trichomes) was counted after 4 weeks of growth in unvernalized plants. Bolting time was recorded as the day on which the inflorescence stem was first visible, corresponding to a bolt of approximately 1 cm. The number of aerial rosettes, inflorescence axillary meristems (IAMs), and leaves on the first AM on the primary inflorescence (first IAM) were counted at five weeks (35 days) after the bolting date in vernalized and unvernalized plants.

RNA isolation and RT-qPCR

For juvenile plants, five 14 day-old seedlings were pooled in 2 ml Eppendorf tubes with a metal bead, snap-frozen in liquid nitrogen and pulverized in the Qiagen Tissuelyser (Qiagen, Hilden, Germany). For bolting plants, the above-ground rosette of 3 plants showing a 1 cm bolt was harvested, leaves and

the emerging inflorescence were removed, and the rosette cores were snap frozen in liquid nitrogen and ground with a mortar and pestle. IAMs (from the central inflorescence and rosette branches) were harvested at 5 weeks after bolting and material of three plants was pooled in a 2 ml Eppendorf tube with a metal bead, snap frozen in liquid nitrogen, and pulverized using the Qiagen Tissuelyser.

RNA was isolated using the RNeasy Plant mini kit (Qiagen, Hilden, Germany). For qPCR analysis, 1 µg of RNA was aliquoted to a fresh tube and treated with DNAse I for 30 minutes to remove any remaining DNA, and used for cDNA synthesis with the RevertAid First Strand Kit (ThermoFisher, Vilnius, Lithuania) according to the supplied protocol. RT-qPCR was performed using TB green ex-taq II (Takara Bio Europe, Saint-Germain-en-Laye, France) in the quantstudio 5 qPCR machine (Invitrogen). Primers used for RT-qPCR are listed in Supplementary table 3 and were synthesized by Sigma Aldrich (Haverhill, United Kingdom).

Data analysis and statistics

All data analysis was performed using R version 4.2.1. (R Core Team, 2023), plots were made with ggplot2 version 3.3.6 (Wickham, 2016) and ggpubr version 0.4.0 (Kassambara, 2023a). Statistical analysis was performed using the packages rstatix version 0.7.0 (Kassambara, 2023b) and agricolae version 1.3.5 (de Mendiburu, 2023). The package psych version 2.3.6 (William Revelle, 2023) was used to calculate Pearson correlation matrices, and heatmaps were plotted with corrplot version 0.92 (Wei and Simko, 2021).

Means between ecotypes were compared using non-parametric tests (Kruskall-Wallis) and significance groups were determined accordingly. Correlations between phenotypes were done by comparing the phenotypic data (bolting time, total number of ARs, total number of IAMs, percentage ARs, and the number of leaves on the first inflorescence IAM) from each individual plant (n = 195). For comparisons to gene expression and the number of juvenile leaves, the mean values of each phenotype or relative expression per genotype were used (n = 13), as the observations from gene expression studies could not be linked to an individual plant, and the number of juvenile leaves was phenotyped in a destructive manner.

For principal component analysis, the average values of phenotypic- or expression data per ecotype were used and the calculations and plots were made in R using the packages FactoMineR version 2.8 (Lê et al., 2008) and factoextra version 1.0.7 (Kassambara and Mundt, 2020).

Acknowledgements

We thank Jan Vink, Ward de Winter and Mariel Lavrijsen for technical support and Kiki Spaninks, Jelmer van Lieshout, and Jihed Chouaref for help with phenotyping. This work was supported the graduate school green top sectors grant (grant nr. GSGT.2019.024) from the Dutch Research Council (NWO) to TL.

Author contributions

TL and RO conceived and designed the study. Phenotyping of the juvenile phase and gene expression studies in juvenile and RBB tissue were done by TL and MK. Phenotyping of AR traits, gene expression studies in IAM tissue, and data analysis were performed by TL. TL and RO interpreted the data and wrote the manuscript.

Literature

Amasino R. (2009). Floral induction and monocarpic versus polycarpic life histories. Genome Biol **10**: 228.

Atwell S., Huang Y.S., Vilhjálmsson B.J., Willems G., Horton M., Li Y., Meng D., Platt A., Tarone A.M., Hu T.T., et al (2010). Genome-wide association study of 107 phenotypes in *Arabidopsis thaliana* inbred lines. Nature 2010 465:7298 **465**: 627–631.

Balanzà V., Martínez-Fernández I., Ferrándiz C. (2014). Sequential action of FRUITFULL as a modulator of the activity of the floral regulators SVP and SOC1. J EXP BOT **65**: 1193–1203.

Davin N., Edger P.P., Hefer C.A., Mizrachi E., Schuetz M., Smets E., Myburg A.A., Douglas C.J., Schranz M.E., Lens F. (2016). Functional network analysis of genes differentially expressed during xylogenesis in *soc1ful* woody *Arabidopsis plants*. The Plant Journal **86**: 376–390.

Deng W., Ying H., Helliwell C.A., Taylor J.M., Peacock W.J., Dennis E.S. (2011). FLOWERING LOCUS C (FLC) regulates development pathways throughout the life cycle of Arabidopsis. PNAS **108**: 6680–6685.

Dorca-Fornell C., Gregis V., Grandi V., Coupland G., Colombo L., Kater M.M. (2011). The Arabidopsis *SOC1*-like genes *AGL42, AGL71* and *AGL72* promote flowering in the shoot apical and axillary meristems. Plant J **67**: 1006–1017.

Duncan S., Holm S., Questa J., Irwin J., Grant A., Dean C. (2015). Seasonal shift in timing of vernalization as an adaptation to extreme winter. Elife **4**: e06620.

Gu X., Le C., Wang Y., Li Z., Jiang D., Wang Y., He Y. (2013). Arabidopsis *FLC* clade members form flowering-repressor complexes coordinating responses to endogenous and environmental cues. Nat Commun **4**: 1–10.

Hu X., Kong X., Wang C., Ma L., Zhao J., Wei J., Zhang X., Loake G.J., Zhang T., Huang J., et al (2014). Proteasome-mediated degradation of FRIGIDA modulates glowering time in Arabidopsis during vernalization. Plant Cell **26**: 4763–4781.

Hyun Y., Richter R., Vincent C., Martinez-Gallegos R., Porri A., Coupland G. (2016). Multi-layered regulation of *SPL15* and cooperation with SOC1 integrate endogenous flowering pathways at the Arabidopsis shoot meristem. Dev Cell **37**: 254–266.

Hyun Y., Vincent C., Tilmes V., Bergonzi S., Kiefer C., Richter R., Martinez-Gallegos R., Severing E., Coupland G. (2019). A regulatory circuit conferring varied flowering response to cold in annual and perennial plants. Science (1979) **363**: 409–412.

Immink R.G.H., Posé D., Ferrario S., Ott F., Kaufmann K., Valentim F.L., de Folter S., van der Wal F., van Dijk A.D.J., Schmid M., et al (2012). Characterization of SOC1's central role in flowering by the identification of its upstream and downstream regulators. Plant Physiol **160**: 433–449.

Johanson U., West J., Lister C., Michaels S., Amasino R., Dean C. (2000). Molecular analysis of *FRIGIDA*, a major determinant of natural variation in Arabidopsis flowering time. Science (1979) **290**: 344–347.

Karami O., Rahimi A., Khan M., Bemer M., Hazarika R.R., Mak P., Compier M.,

van Noort V., Offringa R. (2020). A suppressor of axillary meristem maturation promotes longevity in flowering plants. Nat Plants **6**: 368–376.

Kassambara A. (2023a). ggpubr: "ggplot2" Based Publication Ready Plots.

Kassambara A. (2023b). rstatix: Pipe-Friendly Framework for Basic Statistical Tests.

Kassambara A., Mundt F. (2020). factoextra: Extract and Visualize the Results of Multivariate Data Analyses.

Kiefer C., Bergonzi S., Brand L., Wötzel S., Koch M.A. (2019). Contrasting life history traits in monocarpic versus polycarpic plants from a molecular-evolutionary point of view. Annu Plant Rev **2**: 479–504.

Kiefer C., Severing E., Karl R., Bergonzi S., Koch M., Tresch A., Coupland G. (2017). Divergence of annual and perennial species in the *Brassicaceae* and the contribution of cis-acting variation at *FLC* orthologues. Mol Ecol **26**: 3437–3457.

Kurokura T., Mimida N., Battey N.H., Hytönen T. (2013). The regulation of seasonal flowering in the *Rosaceae*. J EXP BOT **64**: 4131–4141.

Lê S., Josse J., Husson F. (2008). {FactoMineR}: A Package for Multivariate Analysis. J Stat Softw **25**: 1–18.

Melzer S., Lens F., Gennen J., Vanneste S., Rohde A., Beeckman T. (2008). Flowering-time genes modulate meristem determinacy and growth form in *Arabidopsis thaliana*. Nat Genet **40**: 1489–1492.

de Mendiburu F. (2023). agricolae: Statistical Procedures for Agricultural Research.

Ponraj U., Theres K. (2020). Keep a distance to be different: axillary buds initiating at a distance from the shoot apical meristem are crucial for the perennial lifestyle of *Arabis alpina*. New Phytol **227**: 116–131.

R Core Team (2023). R: A Language and Environment for Statistical Computing.

Rahimi A., Karami O., Balazadeh S., Offringa R. (2022). miR156 -independent repression of the ageing pathway by longevity-promoting AHL proteins in Arabidopsis. New Phytol **235**: 2424–2438.

Schwarz S., Grande A. V., Bujdoso N., Saedler H., Huijser P. (2008). The microRNA regulated *SBP*-box genes *SPL9* and *SPL15* control shoot maturation in Arabidopsis. Plant Mol Biol **67**: 183–195.

Tayengwa R., Sharma Koirala P., Pierce C.F., Werner B.E., Neff M.M. (2020). Overexpression of *AtAHL20* causes delayed flowering in Arabidopsis via repression of *FT* expression. BMC Plant Biol **20**: 559.

Teotia S., Lamb R.S. (2009). The paralogous genes *RADICAL-INDUCED CELL DEATH1* and *SIMILAR TO RCD ONE1* have partially redundant functions during Arabidopsis development. Plant Physiol **151**: 180–198.

Thomas H. (2013). Senescence, ageing and death of the whole plant. New Phytol **197**: 696–711.

Tilmes V., Mateos J.L., Madrid E., Vincent C., Severing E., Carrera E., López-Díaz I., Coupland G. (2019). Gibberellins act downstream of *Arabis alpina* PERPETUAL FLOWERING1 to accelerate floral induction during vernalization. Plant Physiol **180**: 1549–1563.

Togninalli M., Seren Ü., Meng D., Fitz J., Nordborg M., Weigel D., Borgwardt

K., Korte A., Grimm D.G. (2018). The AraGWAS Catalog: a curated and standardized *Arabidopsis thaliana* GWAS catalog. Nucleic Acids Res **46**: D1150–D1156.

Vargas-Hernández B.Y., Núñez-Muñoz L., Calderón-Pérez B., Xoconostle-Cázares B., Ruiz-Medrano R. (2022). The NAC transcription factor ANAC087 induces aerial rosette development and leaf senescence in Arabidopsis. Front Plant Sci **13**: 117.

Vayssières A., Mishra P., Roggen A., Neumann U., Ljung K., Albani M.C. (2020). Vernalization shapes shoot architecture and ensures the maintenance of dormant buds in the perennial *Arabis alpina*. New Phytol **227**: 99–115.

Wang Q., Sajja U., Rosloski S., Humphrey T., Kim M.C., Bomblies K., Weigel D., Grbic V. (2007). HUA2 caused natural variation in shoot morphology of *A. thaliana*. Current Biology **17**: 1513–1519.

Wei T., Simko V. (2021). R package "corrplot": Visualization of a Correlation Matrix.

Weigel D., Nilsson O. (1995). A developmental switch sufficient for flower initiation in diverse plants. Nature **377**: 495–500.

Wickham H. (2016). ggplot2: Elegant Graphics for Data Analysis.

William Revelle (2023). psych: Procedures for Psychological, Psychometric, and Personality Research.

Wu G., Poethig R.S. (2006). Temporal regulation of shoot development in *Arabidopsis thaliana* by miR156 and its target *SPL3*. Development **133**: 3539–3547.

Xu M., Hu T., Zhao J., Park M.-Y., Earley K.W., Wu G., Yang L., Poethig R.S. (2016). Developmental functions of miR156-Regulated *SQUAMOSA PROMOTER BINDING PROTEIN-LIKE (SPL)* genes in *Arabidopsis thaliana*. PLOS Genet **12**: e1006263.

Zhai D., Zhang L.-Y., Li L.-Z., Xu Z.-G., Liu X.-L., Shang G.-D., Zhao B., Gao J., Wang F.-X., Wang J.-W. (2024). Reciprocal conversion between annual and polycarpic perennial flowering behavior in the *Brassicaceae*. Cell **187**: 1–19.

Zhang L., Jiménez-Gómez J.M. (2020). Functional analysis of *FRIGIDA* using naturally occurring variation in *Arabidopsis thaliana*. The Plant Journal **103**: 154–165.

Zhao J., Favero D.S., Peng H., Neff M.M. (2013). *Arabidopsis thaliana* AHL family modulates hypocotyl growth redundantly by interacting with each other via the PPC/DUF296 domain. PNAS **110**: E4688–E4697.

Supplementary figures

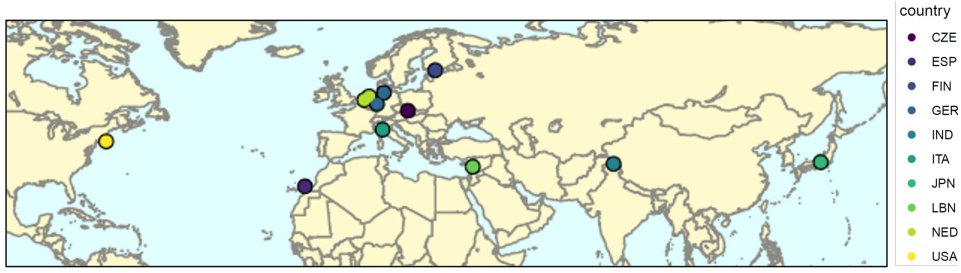

Name	Country	NASC ID
Amel-1	NED	N76434
Br-0	CZE	N76455
Do-0	GER	N76474
Es-0	FIN	N76484
Gifu-2	JPN	N76494
Had-1b	LBN	N76509
Hh-0	GER	N76512
Kas-2	IND	N78905
Mr-0	ITA	N78474
Mv-0	USA	N76556
Tha-1	NED	N76611
Can-0	ESP	N28130

Supplementary Figure 1: Geographical origin of the 12 AR ecotypes. Seeds were retrieved from the Nottingham Arabidopsis Stock Centre (NASC).

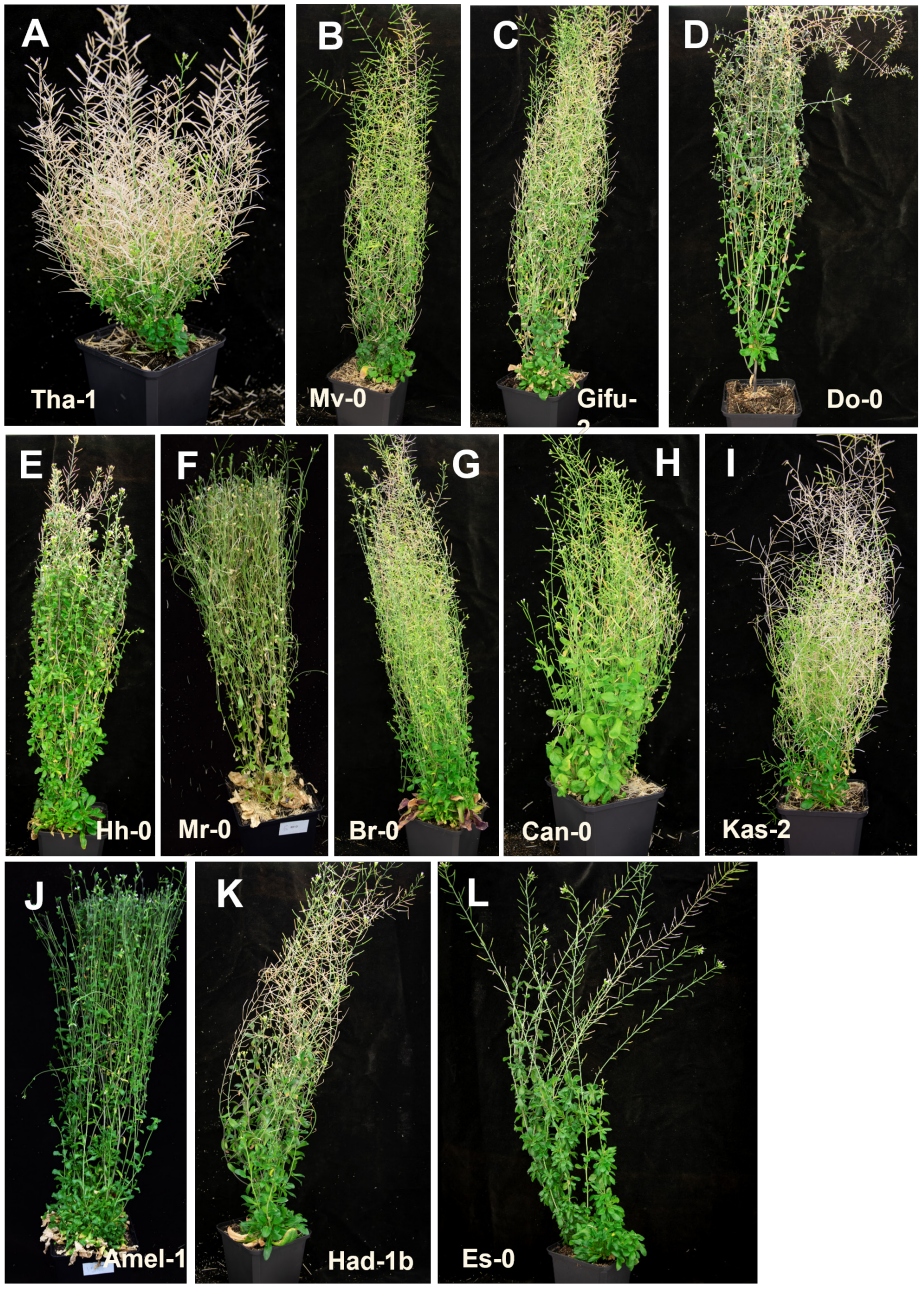

Supplementary figure 2: Phenotypes of 6-month old AR ecotypes grown in long day conditions. The ecotypes are arranged according to the percentage of IAMs forming ARs. Col-0 (not included) had completely senesced at this time point. All pots are 11 cm wide.

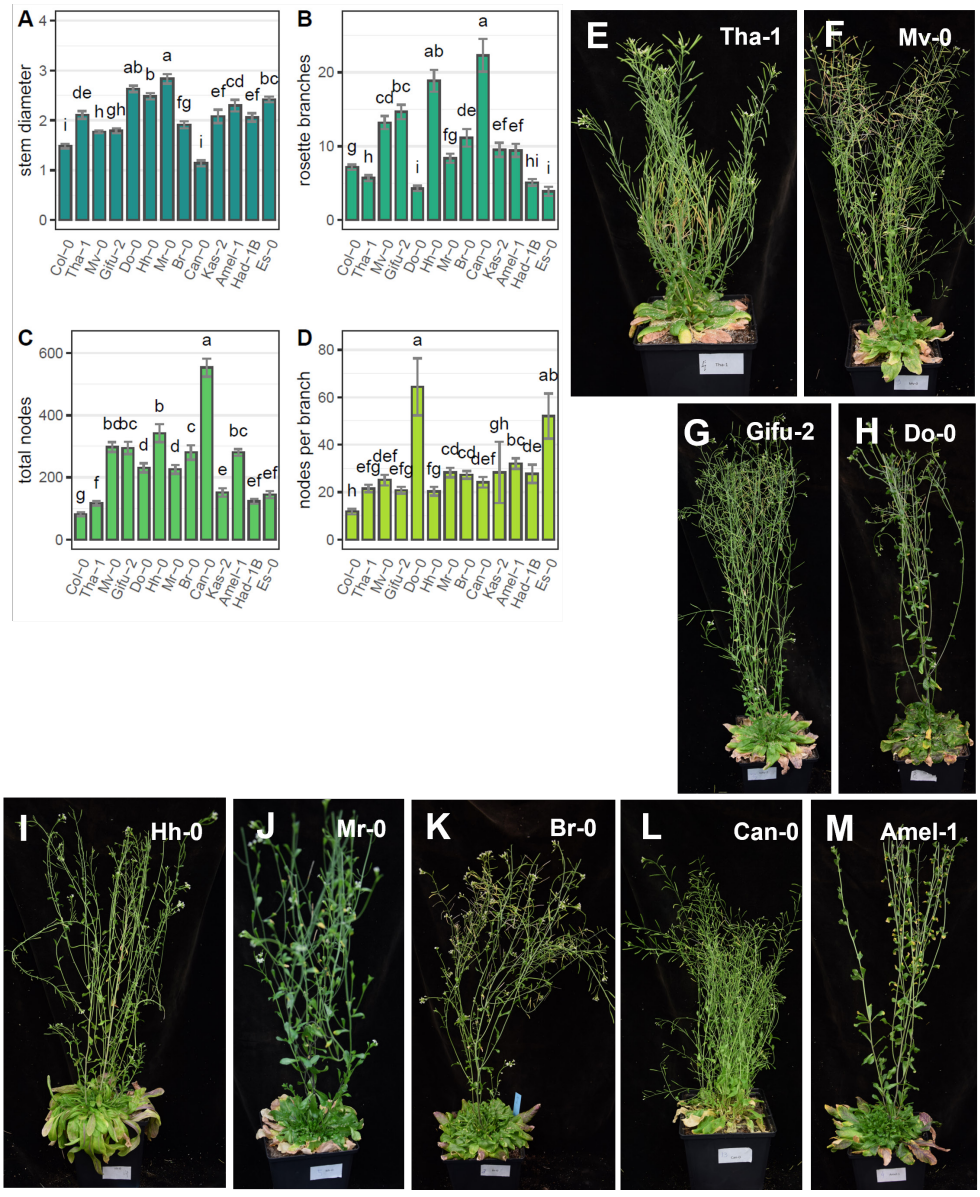

Supplementary figure 3: Phenotypes of AR ecotypes at five weeks after bolting. **A**: the stem diameter below the first node in mm. **B**: the number of rosette branches. **C**: the total number of influencerence axillary mersitems (IAMs). **D**: the number of inflorescence nodes/IAMs per rosette branch (total number of nodes divided by the number of rosette branches). Phenotypes in **A-D** were all measured at five weeks after bolting and were based on measurements in 10-15 plants per ecotype. Measurements were compared between ecotypes with the Kruskall-Wallis test, and significantly different groups are indicated by Chapter 2 different letters. **E-M**: Inflorescence phenotypes of 9 AR ecotypes at five weeks after bolting. All pots have a width of 11 cm.

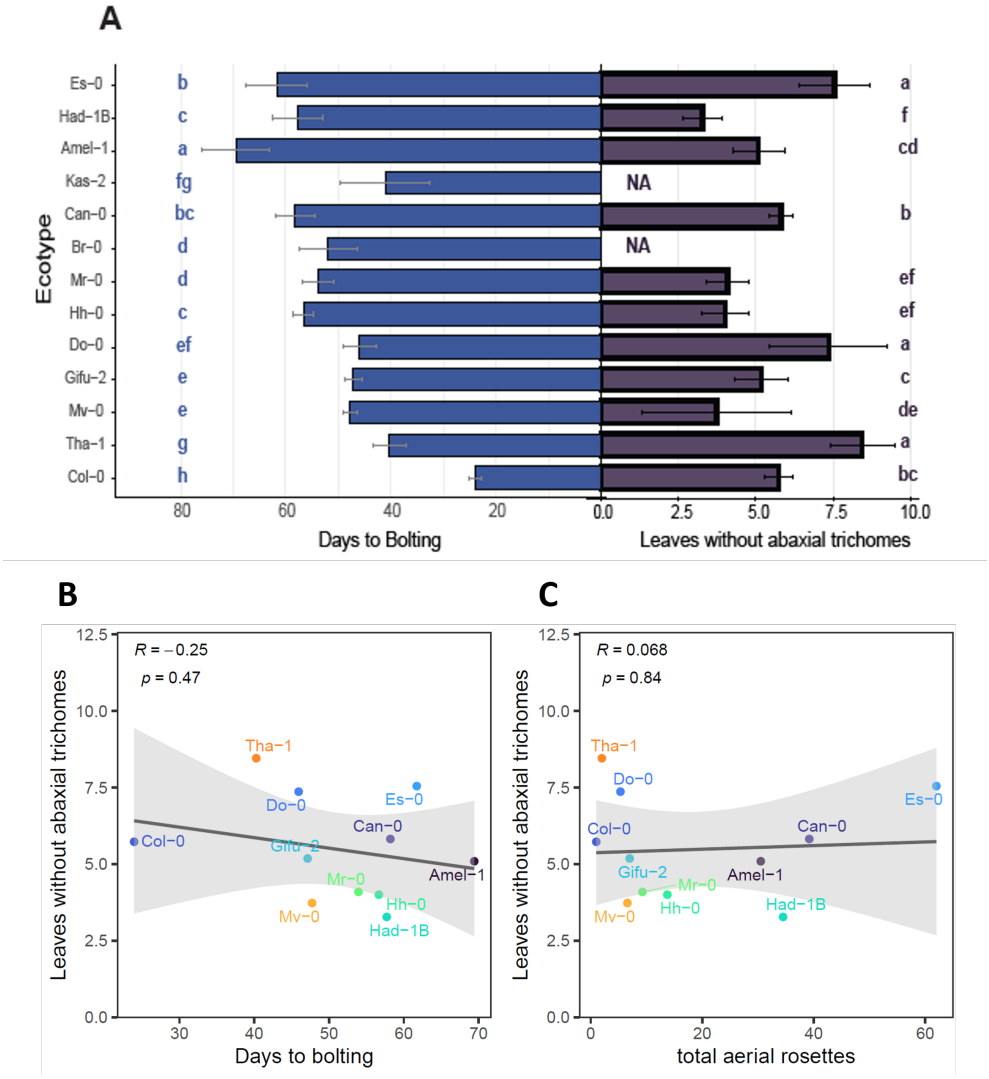

Supplementary figure 4: Juvenile leaves (leaves without abaxial trichomes) in AR ecotypes. **A**: days to bolting and the number of juvenile leaves. Ecotypes Br-0 and Kas-2 do not produce abaxial trichomes on juvenile or adult leaves, and could therefore not be phenotyped for this trait. Measurements were compared between ecotypes with the Kruskall-Wallis test; letters indicate significance groups and error bars show the standard error of the mean. **B-C:** Pearson's correlation between bolting time and juvenile leaf number (**B**) and the total number of aerial rosettes and juvenile leaf number (**C**) showing that bolting time and aerial rosette number do not correlate with the number of juvenile leaves. Measurements in A are based on 10-15 plants each, and average values for each value were entered in the correlation analysis.

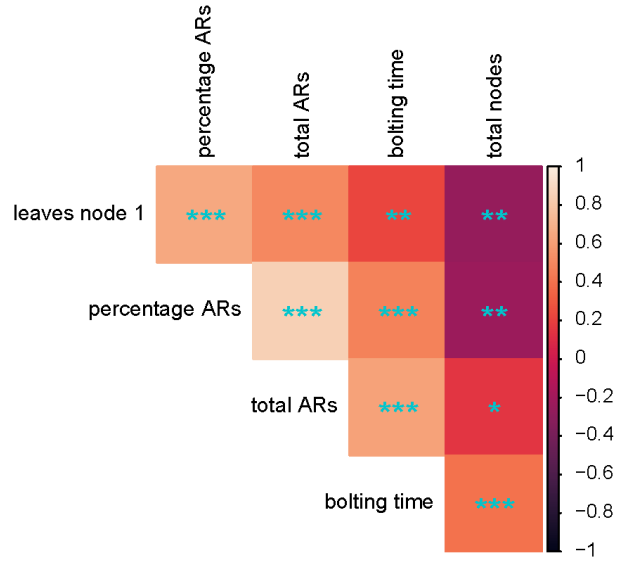

Supplementary figure 5: Heatmap showing Pearson's correlation analysis between phenotypes at five weeks after bolting. Average values for each phenotype were entered in the analyses and were each based on 10-15 plants per ecotype. Blue stars indicate significance levels (*: p<0.05, **: p<0.01, ***: p<0.01) and colors are scaled to Pearson's R.

Supplementary figure 6 (right): Expression of *AHL15, AHL20*, and *FLC* at different developmental stages (juvenile (JUV), rosette base at bolting (RBB), inflorescence axillary meristem (IAM) at five weeks after bolting). **A-C**: Expression of *AHL15* in JUV (**A**), RBB (**B**), and in the IAM (**C**). **D-F**: Expression of *AHL20* in JUV (**D**), RBB (**E**), and in the IAM (**F**). **G**: Comparison of expression of *AHL15* in JUV, RBB, and IAM tissue. **H**: Comparison of expression of *AHL20* in JUV, RBB, and IAM tissue. **I-K**: Expression of *FLC* in JUV (**I**), RBB (**J**), and IAM tissue (**K**). Expression was measured in three samples per ecotype, and each sample consisted of tissue collected from three plants. Differences in expression were calculated between the ecotypes and Col-0 by student's t-test, stars indicate significant differences (*: p<0.05, **: p<0.01) and error bars represent the standard error of the mean.

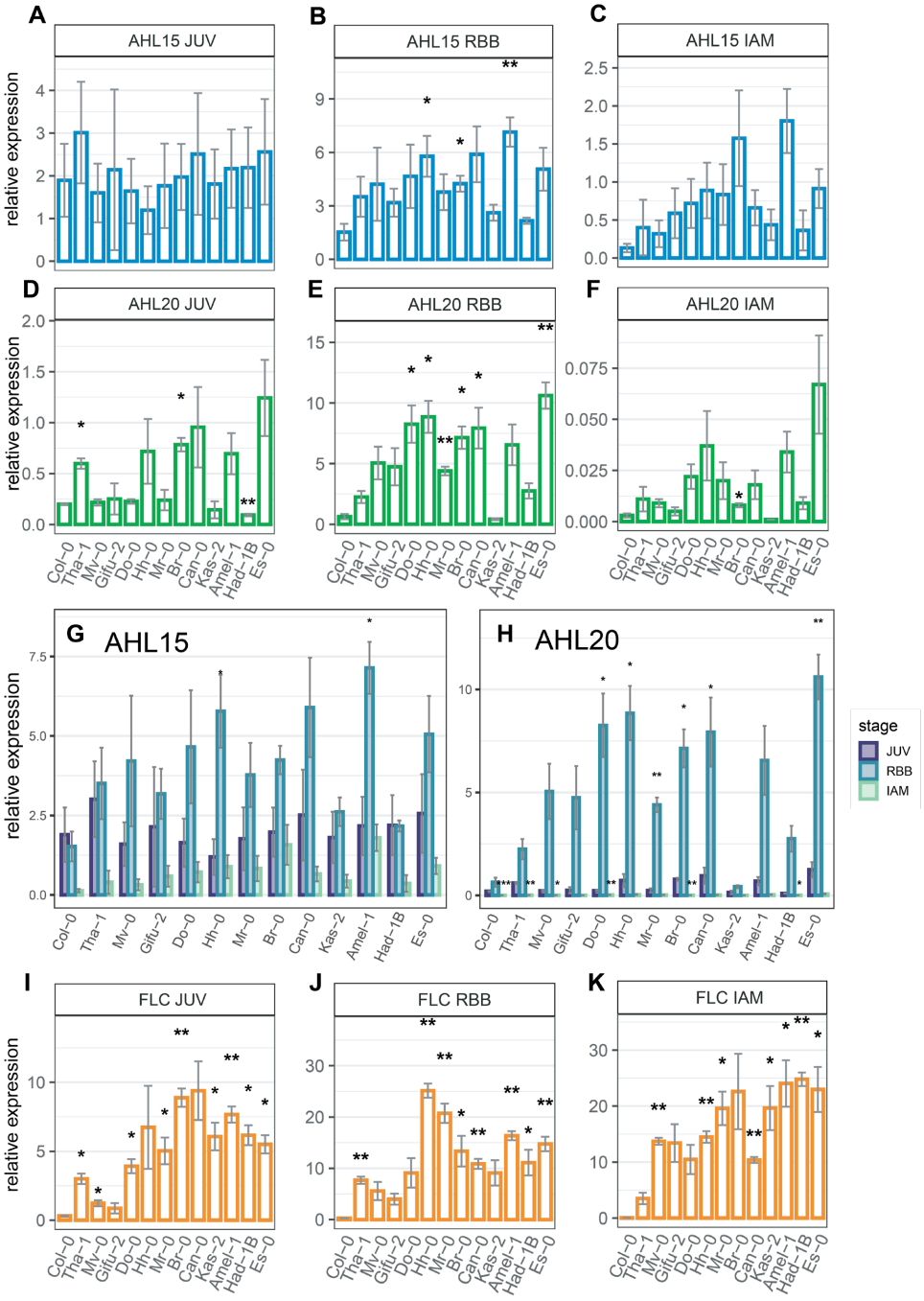
A
AHL15 JUV
B
AHL15 RBB
C
AHL15 IAM
D
AHL20 JUV
E
AHL20 RBB
F
AHL20 IAM
G
AHL15
H
AHL20
I
FLC JUV
J
FLC RBB
K
FLC IAM
relative expression
stage
JUV
RBB
IAM
Col-0
Tha-1
Mv-0
Gifu-2
Do-0
Hh-0
Mr-0
Br-0
Can-0
Kas-2
Amel-1
Had-1B
Es-0

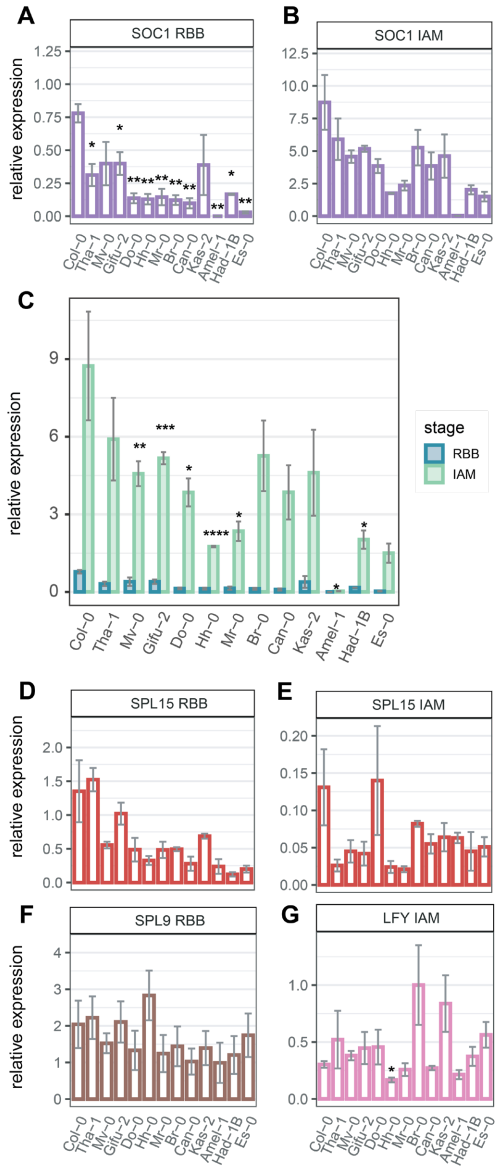

Supplementary figure 7: Expression of *SOC1, SPL15, SPL9* and *LFY* at different developmental stages (Rosette base at bolting (RBB), inflorescence axillary meristem at five weeks after bolting (IAM)). **A-C**: Expression of *SOC1* in the RBB (**A**) or in the IAM (**B**) or both RBB and IAM (**C**). **D-E**: Expression of *SPL15* in the RBB (**D**) or the IAM (**E**). **F**: Expression of *SPL9* in the RBB. **G**: Expression of *LFY* in the IAM. Expression was measured in three samples per ecotype, and each consisted sample of tissue collected from three plants. Differences in expression were calculated between the ecotypes and Col-0 by t-test, stars indicate significant differences (*: p<0.05, **: p<0.01, ***: p<0.001), and error bars show the standard error of the mean.

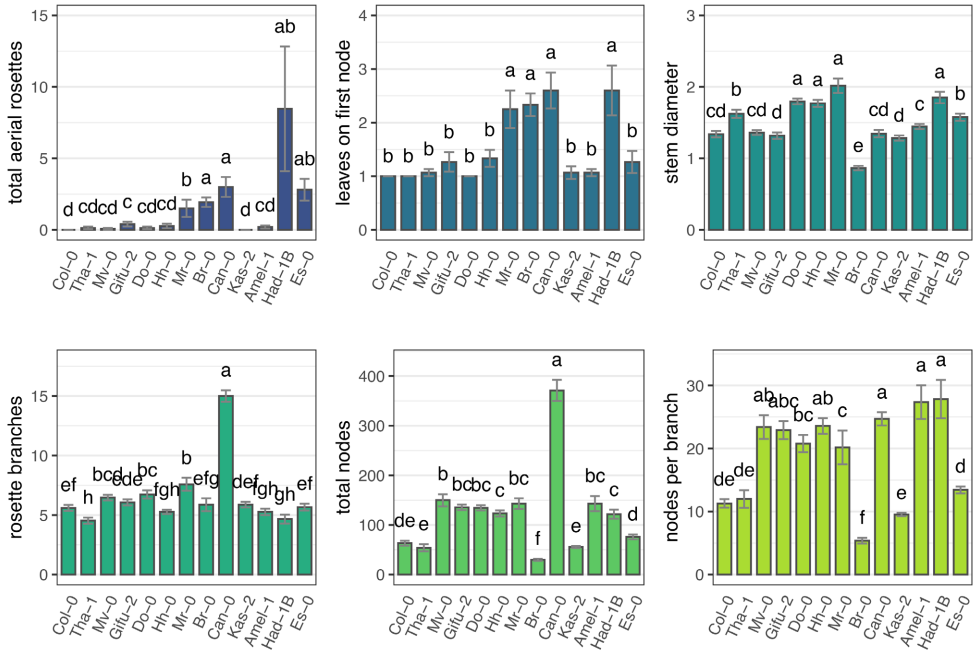

Supplementary figure 8: Phenotypic analysis of vernalized plants at five weeks after bolting. **A**: The total number of inflorescence nodes bearing three or more cauline leaves (ARs). **B**: The number of leaves on the first inflorescence node. **C**: The diameter of the central stem beneath the first inflorescence node in mm. **D**: The number of rosette branches. **E**: The total number of inflorescence nodes/AMs. **F**: The number of inflorescence nodes per branch, calculated by dividing the total number of nodes by the total number of rosette branches. For each phenotypic trait, 10-15 plants per ecotype were measured. Measurements between ecotypes were compared by Kruskall-Wallis test. Significantly different groups are indicated by different letters and error bars show the standard error of the mean.

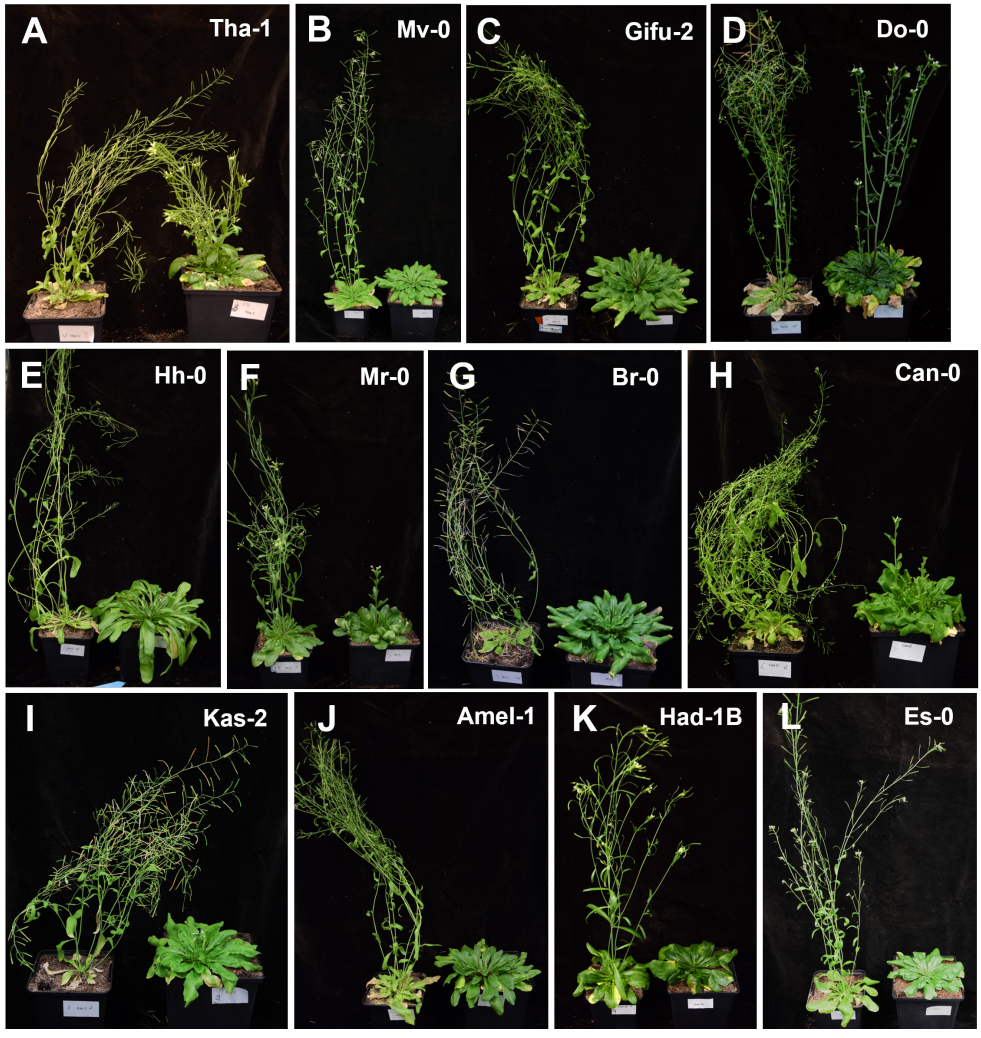

Supplementary figure 9: Phenotypes of vernalized AR ecotypes at five weeks after bolting (left) and non-vernalized plants of the same ecotype at the same age (right). Ecotypes are arranged by ascending percentage of ARs at five weeks after bolting in non-vernalized conditions. Pots of vernalized plants (left) are 9 cm wide and pots of non-vernalized plants (right) are 11 cm wide.

Supplementary data

Supplementary table 1: Pearson's correlation coefficients between phenotypic and gene expression data in non-vernalized ecotypes. Significant negative correlations are indicated in blue and significant positive correlations are given in red.

variable 1	variable 2	*R*	R^2	*p*
bolting time	SOC1 IAM	**-0.92**	0.85	0.000007
bolting time	SOC1 RBB	**-0.91**	0.83	0.000016
total ARs	percentage ARs	**0.88**	0.78	0.000070
leaves node 1	percentage ARs	**0.88**	0.77	0.000074
SOC1 IAM	SOC1 RBB	**0.85**	0.72	0.000239
bolting time	SPL15 RBB	**-0.83**	0.69	0.000455
SOC1 IAM	SPL15 RBB	**0.82**	0.67	0.000625
AHL20 IAM	AHL20 RBB	**0.80**	0.63	0.001137
AHL15 RBB	AHL20 RBB	**0.79**	0.62	0.001457
FLC IAM	SPL15 RBB	**-0.78**	0.60	0.001762
SOC1 IAM	FLC RBB	**-0.77**	0.60	0.001868
AHL20 IAM	AHL15 RBB	**0.77**	0.59	0.002249
SPL15 RBB	SOC1 RBB	**0.77**	0.59	0.002306
bolting time	FLC IAM	**0.76**	0.58	0.002574
bolting time	AHL15 RBB	**0.76**	0.57	0.002719
AHL15 RBB	SOC1 RBB	**-0.75**	0.57	0.003011
FLC IAM	SOC1 IAM	**-0.75**	0.56	0.003215
FLC RBB	SOC1 RBB	**-0.75**	0.56	0.003396
AHL20 IAM	SOC1 IAM	**-0.74**	0.55	0.003754
AHL20 RBB	SOC1 RBB	**-0.73**	0.54	0.004234
AHL20 IAM	FLC RBB	**0.71**	0.50	0.006837
AHL20 IAM	SOC1 RBB	**-0.70**	0.49	0.007409
AHL15 IAM	AHL15 RBB	**0.70**	0.49	0.007524
bolting time	FLC RBB	**0.70**	0.48	0.008220
bolting time	total ARs	**0.69**	0.48	0.008656
bolting time	AHL20 IAM	**0.69**	0.48	0.009014
total ARs	leaves node 1	**0.69**	0.48	0.009055
total ARs	SPL15 RBB	**-0.68**	0.47	0.010245
FLC IAM	SOC1 RBB	**-0.67**	0.45	0.011443
AHL15 IAM	SOC1 RBB	**-0.67**	0.45	0.011969
bolting time	AHL20 RBB	**0.67**	0.45	0.012265
SOC1 IAM	AHL15 RBB	**-0.67**	0.45	0.012596
percentage ARs	FLC IAM	**0.67**	0.45	0.012694
bolting time	AHL15 IAM	**0.65**	0.43	0.015347
total nodes	AHL15 RBB	**0.65**	0.42	0.015788
total ARs	FLC IAM	**0.65**	0.42	0.016543
FLC RBB	SPL15 RBB	**-0.62**	0.39	0.022478
AHL20 RBB	SPL15 RBB	**-0.62**	0.39	0.023480
leaves node 1	FLC IAM	**0.61**	0.37	0.026699
total ARs	SOC1 RBB	**-0.61**	0.37	0.027645
AHL15 RBB	FLC RBB	**0.60**	0.36	0.031237
total ARs	SOC1 IAM	**-0.59**	0.35	0.032747
total ARs	AHL20 IAM	**0.58**	0.34	0.036836
AHL15 IAM	FLC RBB	**0.57**	0.32	0.042782

AHL20 IAM	SPL15 RBB	**-0.56**	0.31	0.047552
SOC1 IAM	AHL20 RBB	-0.55	0.30	0.050741
AHL15 RBB	SPL15 RBB	-0.55	0.30	0.051516
FLC IAM	FLC RBB	0.54	0.29	0.056104
FLC RBB	AHL20 RBB	0.54	0.29	0.058275
AHL15 IAM	FLC IAM	0.54	0.29	0.058622
AHL15 IAM	SOC1 IAM	-0.54	0.29	0.058622
total nodes	AHL20 RBB	0.54	0.29	0.059483
percentage ARs	SPL15 RBB	-0.53	0.28	0.061831
total ARs	AHL20 RBB	0.52	0.27	0.066967
AHL15 IAM	AHL20 RBB	0.51	0.26	0.073259
leaves node 1	AHL20 IAM	0.49	0.24	0.085683
percentage ARs	SOC1 IAM	-0.49	0.24	0.085863
bolting time	percentage ARs	0.49	0.24	0.088578
SPL9 RBB	SPL15 RBB	0.49	0.24	0.090275
SPL15 IAM	FLC RBB	-0.48	0.23	0.095469
percentage ARs	AHL20 IAM	0.48	0.23	0.096703
AHL15 IAM	AHL20 IAM	0.47	0.22	0.109286
bolting time	SPL15 IAM	-0.46	0.21	0.115731
bolting time	total nodes	0.46	0.21	0.117051
AHL15 IAM	SPL15 RBB	-0.45	0.20	0.120279
leaves node 1	SOC1 IAM	-0.44	0.19	0.132496
SOC1 IAM	SPL15 IAM	0.44	0.19	0.134263
leaves node 1	SPL15 RBB	-0.44	0.19	0.136517
percentage ARs	SOC1 RBB	-0.43	0.19	0.140733
FLC IAM	SPL9 RBB	-0.43	0.19	0.141592
leaves node 1	SOC1 RBB	-0.43	0.18	0.143615
total nodes	SPL15 RBB	-0.41	0.17	0.166515
total ARs	AHL15 RBB	0.41	0.17	0.167474
total nodes	SOC1 RBB	-0.40	0.16	0.172873
AHL20 IAM	FLC IAM	0.39	0.15	0.188801
leaves node 1	FLC RBB	0.37	0.14	0.210644
leaves node 1	total nodes	-0.37	0.14	0.212089
bolting time	SPL9 RBB	-0.37	0.14	0.214437
FLC IAM	AHL20 RBB	0.36	0.13	0.229296
SPL9 RBB	SOC1 RBB	0.36	0.13	0.230107
leaves node 1	LFY IAM	0.36	0.13	0.233347
total ARs	SPL9 RBB	-0.35	0.12	0.245555
bolting time	leaves node 1	0.34	0.12	0.251103
total nodes	AHL15 IAM	0.33	0.11	0.265257
percentage ARs	AHL20 RBB	0.33	0.11	0.270420
total ARs	FLC RBB	0.33	0.11	0.272554
SPL15 IAM	SOC1 RBB	0.33	0.11	0.274754
leaves node 1	AHL20 RBB	0.32	0.10	0.288613
FLC IAM	SPL15 IAM	-0.32	0.10	0.289916
AHL20 IAM	LFY IAM	-0.31	0.10	0.295563
FLC IAM	AHL15 RBB	0.30	0.09	0.319850
SOC1 IAM	SPL9 RBB	0.30	0.09	0.320981
FLC IAM	LFY IAM	0.29	0.08	0.337974
SOC1 IAM	LFY IAM	0.29	0.08	0.343096

AHL15 IAM	SPL9 RBB	-0.28	0.08	0.346542
total nodes	LFY IAM	-0.28	0.08	0.353776
total nodes	FLC RBB	0.27	0.07	0.365457
total nodes	percentage ARs	-0.27	0.07	0.367042
LFY IAM	AHL15 RBB	-0.27	0.07	0.378106
total nodes	SOC1 IAM	-0.25	0.06	0.406558
total ARs	AHL15 IAM	0.24	0.06	0.423353
percentage ARs	FLC RBB	0.22	0.05	0.467809
percentage ARs	LFY IAM	0.21	0.04	0.496996
SPL15 IAM	SPL9 RBB	-0.20	0.04	0.507845
total nodes	AHL20 IAM	0.20	0.04	0.510321
total ARs	SPL15 IAM	-0.20	0.04	0.510530
LFY IAM	FLC RBB	-0.20	0.04	0.510959
AHL20 IAM	SPL15 IAM	-0.20	0.04	0.511028
total nodes	SPL15 IAM	-0.20	0.04	0.518925
percentage ARs	SPL9 RBB	-0.20	0.04	0.522352
SPL15 IAM	AHL15 RBB	-0.19	0.04	0.533598
total nodes	SPL9 RBB	-0.19	0.03	0.543956
LFY IAM	SPL15 IAM	0.17	0.03	0.570269
bolting time	LFY IAM	-0.17	0.03	0.573146
percentage ARs	SPL15 IAM	-0.17	0.03	0.580095
leaves node 1	SPL15 IAM	-0.17	0.03	0.583464
total ARs	total nodes	0.16	0.03	0.600188
AHL15 RBB	SPL9 RBB	-0.16	0.03	0.600703
SPL15 IAM	SPL15 RBB	0.15	0.02	0.618937
AHL15 IAM	LFY IAM	0.12	0.01	0.701505
LFY IAM	SPL9 RBB	-0.10	0.01	0.750270
LFY IAM	SPL15 RBB	0.10	0.01	0.753373
AHL20 IAM	SPL9 RBB	0.08	0.01	0.792394
total ARs	LFY IAM	0.08	0.01	0.796683
percentage ARs	AHL15 RBB	0.08	0.01	0.804599
LFY IAM	AHL20 RBB	-0.07	0.00	0.822797
SPL15 IAM	AHL20 RBB	-0.05	0.00	0.860349
leaves node 1	SPL9 RBB	-0.05	0.00	0.873601
FLC RBB	SPL9 RBB	0.04	0.00	0.901335
AHL15 IAM	SPL15 IAM	-0.03	0.00	0.916355
percentage ARs	AHL15 IAM	0.03	0.00	0.931908
leaves node 1	AHL15 RBB	0.02	0.00	0.947784
leaves node 1	AHL15 IAM	-0.01	0.00	0.977059
total nodes	FLC IAM	0.01	0.00	0.977901
AHL20 RBB	SPL9 RBB	-0.01	0.00	0.982716
LFY IAM	SOC1 RBB	0.00	0.00	0.995843

Supplementary table 2A: contributions of phenotype- and gene expression variables to the principal component analysis shown in Figure 4.

Variable	Dim.1	Dim.2	Dim.3	Dim.4	Dim.5
SOC1_RBB	14.11	0.54	0.00	0.29	0.45
SOC1_IAM	13.72	0.06	4.30	3.14	0.65
SPL15_RBB	11.46	3.66	0.33	6.48	11.76
FLC_RBB	10.77	3.10	4.50	2.27	0.86
AHL15_RBB	10.60	2.61	8.78	0.17	18.04
AHL20_RBB	9.65	2.59	16.33	1.41	5.01
AHL20_IAM	8.85	7.14	4.46	0.65	20.90
AHL15_IAM	8.80	3.10	4.82	7.91	28.47
FLC_IAM	8.41	13.93	10.33	1.24	4.16
SPL15_IAM	1.86	7.21	45.87	3.02	4.02
SPL9_RBB	1.33	32.35	0.07	24.78	3.10
LFY_IAM	0.46	23.71	0.21	48.63	2.61

Supplementary table 2B: Contributions of the individual ecotypes to the principal component analysis shown in Figure 4.

Ecotype	Dim.1	Dim.2	Dim.3	Dim.4	Dim.5
Col-0	38.26	1.77	9.27	3.60	0.75
Amel-1	18.18	1.16	1.64	5.46	25.52
Es-0	12.50	1.03	2.65	5.28	39.03
Tha-1	8.89	9.06	1.49	8.66	9.58
Hh-0	7.54	39.71	0.92	4.53	0.24
Gifu-2	4.62	1.15	0.81	2.11	0.43
Kas-2	4.07	14.89	8.07	2.83	0.89
Mr-0	2.21	0.09	14.22	2.59	2.33
Mv-0	1.47	0.05	0.66	3.60	0.16
Can-0	1.40	0.07	3.01	12.94	3.15
Br-0	0.75	22.92	3.71	34.81	3.69
Had-1B	0.07	6.67	22.16	9.88	11.28
Do-0	0.04	1.44	31.38	3.70	2.94

Supplementary table 3: RT-qPCR primers used to measure gene expression in this study.

name*	sequence (5' to 3')	function
PP2A-3-Q-fw	ACGTGGCCAAAATGATGCAA	reference gene for RT-qPCR
PP2A-3-Q-rev	TCATGTTCTCCACAACCGCT	reference gene for RT-qPCR
AHL15-Q-fw	CTGAGCGGTAGTGGTTTGGT	RT-qPCR of AHL15
AHL15-Q-rev	AGGAGAGCCAGACGTAGGAA	RT-qPCR of AHL15
AHL20-Q-fw	GGCGGCTCAAGACAGATTCA	RT-qPCR of AHL20
AHL20-Q-rev	AGTAAGGTGGTCTTGCGTGG	RT-qPCR of AHL20
AHL19 Q-fw	CTCTAACGCGACTTACGAGAGATT	RT-qPCR of AHL19
AHL19 Q-rev	ATATTATACACCGGAAGTCCTTGGT	RT-qPCR of AHL19
FLC Q-fw	TGACTAGAGCCAAGAAGACCG	RT-qPCR of FLC
FLC Q-rev	AGTCACCGGAAGATTGTCGG	RT-qPCR of FLC
SOC1 Q-fw	AGCTGCAGAAAACGAGAAGC	RT-qPCR of SOC1
SOC1 Q-rev	TGAAGAACAAGGTAACCCAATG	RT-qPCR of SOC1
LFY-Q-fw	TCATTTGCTACTCTCCGCCG	RT-qPCR of LFY
LFY-Q-rev	CGGTTCCTCAGATAACCCTGT	RT-qPCR of LFY
SPL9-Q-fw	AATTGGCGACTCAAACTGTG	RT-qPCR of SPL9
SPL9-Q-rev	CTGAAGAAGCTCGCCATGTA	RT-qPCR of SPL9
SPL15-Q-fw	TGAATGTTTTATCACATGGAAGCTC	RT-qPCR of SPL15
SPL15-Q-rev	TCATCGAGTCGAAACCAGAAGATG	RT-qPCR of SPL15

* fw: forward, rev: reverse